CSIRO

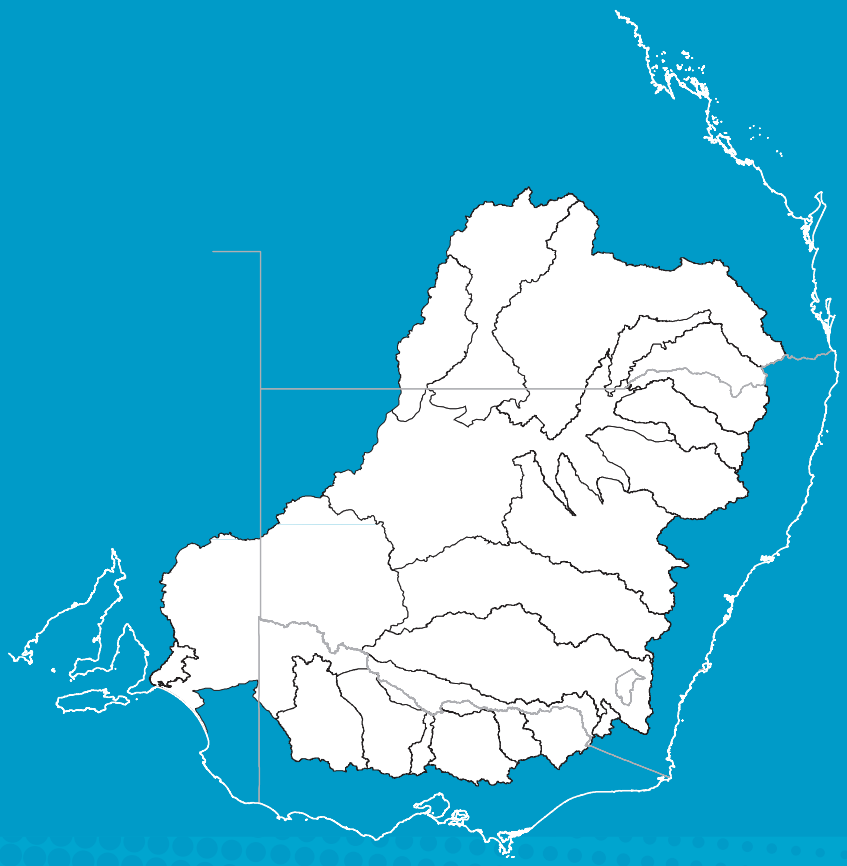

Climate data for hydrologic scenario modelling across the Murray-Darling Basin

A report to the Australian Government from the CSIRO Murray-Darling Basin Sustainable Yields Project

Francis Chiew, Jin Teng, Dewi Kirono, Andrew Frost, Janice Bathols, Jai Vaze, Neil Viney, Kevin Hennessy and Wenju Cai

June 2008

Murray-Darling Basin Sustainable Yields Project acknowledgments

The Murray-Darling Basin Sustainable Yields project is being undertaken by CSIRO under the Australian Government's Raising National Water Standards Program, administered by the National Water Commission. Important aspects of the work were undertaken by Sinclair Knight Merz; Resource & Environmental Management Pty Ltd; Department of Water and Energy (New South Wales); Department of Natural Resources and Water (Queensland); Murray-Darling Basin Commission; Department of Water, Land and Biodiversity Conservation (South Australia); Bureau of Rural Sciences; Salient Solutions Australia Pty Ltd; eWater Cooperative Research Centre; University of Melbourne; Webb, McKeown and Associates Pty Ltd; and several individual sub-contractors.

Acknowledgements

The authors wish to thank Prof Roger Grayson, etc who provided technical review of the report, and Becky Schmidt, CSIRO, for her copy-editing.

Citation

Chiew FHS, Teng J, Kirono D, Frost AJ, Bathols JM, Vaze J, Viney NR, Young WJ, Hennessy KJ and Cai WJ (2008) Climate data for hydrologic scenario modelling across the Murray-Darling Basin. A report to the Australian Government from the CSIRO Murray-Darling Basin Sustainable Yields Project. CSIRO, Australia. 35pp.

Publication Details

ISSN 1835-095X

Preface

This is a report to the Australian Government from CSIRO. It is an output of the Murray-Darling Basin Sustainable Yields Project which assessed current and potential future water availability in 18 regions across the Murray-Darling Basin (MDB) considering climate change and other risks to water resources. The project was commissioned following the Murray-Darling Basin Water Summit convened by the Prime Minister of Australia in November 2006 to report progressively during the latter half of 2007. The reports for each of the 18 regions and for the entire MDB are supported by a series of technical reports detailing the modelling and assessment methods used in the project. This report is one of the supporting technical reports of the project. Project reports can be accessed at http://www.csiro.au/mdbsy.

Project findings are expected to inform the establishment of a new sustainable diversion limit for surface and groundwater in the MDB – one of the responsibilities of a new Murray-Darling Basin Authority in formulating a new Murray-Darling Basin Plan, as required under the Commonwealth Water Act 2007. These reforms are a component of the Australian Government's new national water plan 'Water for our Future'. Amongst other objectives, the national water plan seeks to (i) address over-allocation in the MDB, helping to put it back on a sustainable track, significantly improving the health of rivers and wetlands of the MDB and bringing substantial benefits to irrigators and the community; and (ii) facilitate the modernisation of Australian irrigation, helping to put it on a more sustainable footing against the background of declining water resources.

Summary

This report is one in a series of technical reports from the CSIRO Murray-Darling Basin Sustainable Yields Project. This report describes the climate data for the three climate scenarios used for the hydrological modelling in the project. The three climate scenarios are historical climate, recent climate, and future climate. All three climate scenarios have 112 years of daily climate data for 0.05^{o} x 0.05^{o} (5 km x 5 km) grid cells across the Murray-Darling Basin (MDB).

The historical climate scenario (Scenario A) is the baseline against which other scenarios are compared. It is based on observed SILO Data Drill climate data from 1895 to 2006. The recent climate scenario (Scenario B) is used to assess future water availability should the climate in the future prove to be similar to that of the last ten years. Climate data for 1997 to 2006 are used to generate stochastic replicates of 112-year daily climate sequences. The replicate which produces a mean annual runoff closest to that observed in 1997 to 2006 is selected to define this scenario. The future climate scenario (Scenario C) is used to assess the range of likely climate conditions around the year 2030. Forty-five future climate variants, each with 112 years of daily climate sequences, are used. The future climate variants come from scaling the 1895 to 2006 climate data to represent ~2030 climate, based on analyses of 15 global climate models (GCMs) and three global warming scenarios from the Fourth Assessment Report of the Intergovernmental Panel on Climate Change (IPCC AR4).

The mean annual rainfall, averaged over 1895 to 2006, over the entire MDB is 457 mm. There is a clear east-west rainfall gradient, where rainfall is highest in the south-east (mean annual rainfall of more than 1500 mm) and along the eastern perimeter, and lowest in the west (less than 300 mm). In the northern MDB, most of the rainfall occurs in the summer half of the year, and in the southernmost MDB, most of the rainfall occurs in the winter half of the year. The mean annual areal potential evapotranspiration averaged across the MDB is 1443 mm, varying from 1700 mm in the north to 1000 mm in the south.

The mean annual rainfall averaged over the MDB in the past ten years (1997 to 2006) is 440 mm, which is 4 percent lower than the 1895 to 2006 mean. However, rainfall over the past ten years in the southern MDB is significantly lower than the long-term mean, by up to 15 percent lower in the southernmost parts.

There is considerable uncertainty in the global warming projections and in the predictions of how global warming affects local rainfall. There are very significant differences in the future rainfall projections between the 15 GCMs.

However, the majority of the GCMs shows a decrease in future mean annual rainfall. The best estimate or median indicates that the future mean annual rainfall in the MDB in ~2030 relative to ~1990 will be lower by about 2 percent in the north to 5 percent in the south. Averaged across the MDB, the best estimate or median is a 2.8 percent decrease in mean annual rainfall. The extreme dry and extreme wet estimates in the northern half of the MDB range from a 10 to 15 percent decrease to a 10 to 15 percent increase in mean annual rainfall. In the southern half of the MDB, the extreme estimates range from a 15 to 20 percent decrease in mean annual rainfall to a 5 to 10 percent increase in mean annual rainfall, and in the southernmost parts, the extreme estimates range from a decrease in mean annual rainfall of about 20 percent to little change in mean annual rainfall. Averaged across the MDB, the extreme estimates range from a 13 percent decrease to an 8 percent increase in mean annual rainfall. Most of the GCMs indicate that future winter rainfall is likely to be lower across the MDB. Most of the rainfall and runoff in the southern MDB occur in the winter half of the year, and almost all the GCMs indicate lower future winter rainfall there.

Table of Contents

Tables

Figures

1 Introduction

This report is one in a series of technical reports from the CSIRO Murray-Darling Basin Sustainable Yields Project. The terms of reference for the project are to estimate current and future water availability in each catchment and aquifer in the Murray-Darling Basin (MDB) considering climate change, other risks, and surface-groundwater interactions; and compare the estimated current and future water availability to that required to meet the current levels of extractive use. Results from the project have been reported progressively for 18 contiguous regions across the entire MDB.

The purpose of this report is to describe in more detail the three climate scenarios used for the hydrological modelling in the project. The three climate scenarios are historical climate, recent climate, and future climate. All three climate scenarios have 112 years of daily climate data.

The historical climate scenario (Scenario A) is the baseline against which other scenarios are compared. It is based on observed climate from 1895 to 2006. The historical climate data are described in Chapter 2.

The recent climate scenario (Scenario B) is used to assess future water availability should the climate in the future prove to be similar to that of the last ten years. Climate data for 1997 to 2006 are used to generate stochastic replicates of 112-year daily climate sequences. The replicate which produces a mean annual runoff closest to that observed in 1997 to 2006 is selected to define this scenario. The recent climate scenario is described in Chapter 3.

The future climate scenario (Scenario C) is used to assess the range of likely climate conditions around the year 2030. Forty-five future climate variants, each with 112 years of daily climate sequences, are used. The future climate variants come from scaling the 1895 to 2006 climate data to represent ~2030 climate, based on analyses of 15 global climate models (GCMs) and three global warming scenarios. The future climate scenario is described in Chapter 4.

The Scenario A data described in this report are used for the rainfall-runoff modelling. The Scenario A data used for the river system and groundwater recharge modelling are described elsewhere. The methods used to obtain the Scenario B and Scenario C data, as described in this report, are the same for the rainfall-runoff, river system and groundwater recharge modelling.

2 Historical climate data (Scenario A)

2.1 Gridded historical climate data

Historical daily climate data from 1895 to 2006 for 0.05^{o} x 0.05^{o} (~ 5 km x 5 km) grid cells across the Murray-Darling Basin (MDB) are used. The source of the data is the SILO Data Drill of the Queensland Department of Natural Resources and Water (http://www.nrw.qld.gov.au/silo and Jeffrey et al., 2001). The SILO Data Drill provides surfaces of daily rainfall and other climate data interpolated from point measurements made by the Australian Bureau of Meteorology.

The rainfall surfaces are interpolated using a trivariate thin plate smoothing spline with latitude, longitude and elevation as independent variables. The other climate surfaces after 1957 are also interpolated using the same method, but a different interpolation algorithm is used prior to 1957 because most of the available data before 1957 are not in digital format (see http://www.nrw.qld.gov.au/silo/CLIMARC).

The gridded climate data is derived from observations that have been quality checked by the Australian Bureau of Meteorology and have been subject to error checking by the Queensland Department of Natural Resources and Water. Nevertheless, it is inevitable that there will still be errors in the data and the interpolation routines can also introduce errors. In general, the data accuracy is expected to be lower in areas where the observation density is low relative to the climate gradients. In this context, it should be noted that rainfall varies spatially more than the other climate variables, but this is compensated by the generally denser rainfall observation network.

2.2 Rainfall

Figure 2-1 shows the mean annual, summer (December-January-February), and winter (June-July-August) rainfall across the MDB. The mean annual rainfall averaged over the MDB is 457 mm. There is a clear east–west rainfall gradient across the MDB, where rainfall is highest in the south-east (mean annual rainfall of more than 1500 mm) and along the eastern perimeter, and lowest in the west (mean annual rainfall of less than 300 mm). In the northern MDB, most of the rainfall occurs in the summer half of the year, and in the southernmost MDB, most of the rainfall occurs in the winter half of the year. Potter et al. (2008) provide a detailed discussion of annual rainfall characteristics across the MDB.

Rainfall is the most important driver of the rainfall-runoff model. Rainfall is also much more variable, both temporally and spatially, compared to the other climate variables. Figure 2-2 shows the density of rainfall stations used to generate the SILO Data Drill rainfall data for various decades of the 20^{th} century (stations shown in the plots have more than 2000 daily recorded values over the decade, that is, more than 55 percent of the data). Overall, more than 1400 stations have operated at various times in the MDB. There are more than 1000 stations reporting at least 55 percent of days in a decade for every decade between the 1920s and 1980s, with a peak of 1150 stations in the 1960s. Since the 1960s, the number of reporting stations has declined and by the 1990s, only about 900 stations reported at least 55 percent of days. Most of the increase in stations between the 1900s and 1960s occurred in the south and east. In contrast, the decrease in station density since the 1960s has occurred throughout the MDB.

There is good coverage of rainfall stations in the south and east of the MDB where most of the runoff comes from, and sparser coverage in the north-west where there is little runoff. The relative paucity of rainfall stations in the less populated, mountainous and extreme high rainfall areas in the far south-east is of some concern because this area generates substantial runoff and is characterised by large spatial rainfall gradients. Nevertheless, the SILO Data Drill rainfall remains the best and most readily available source of gridded data for the project.

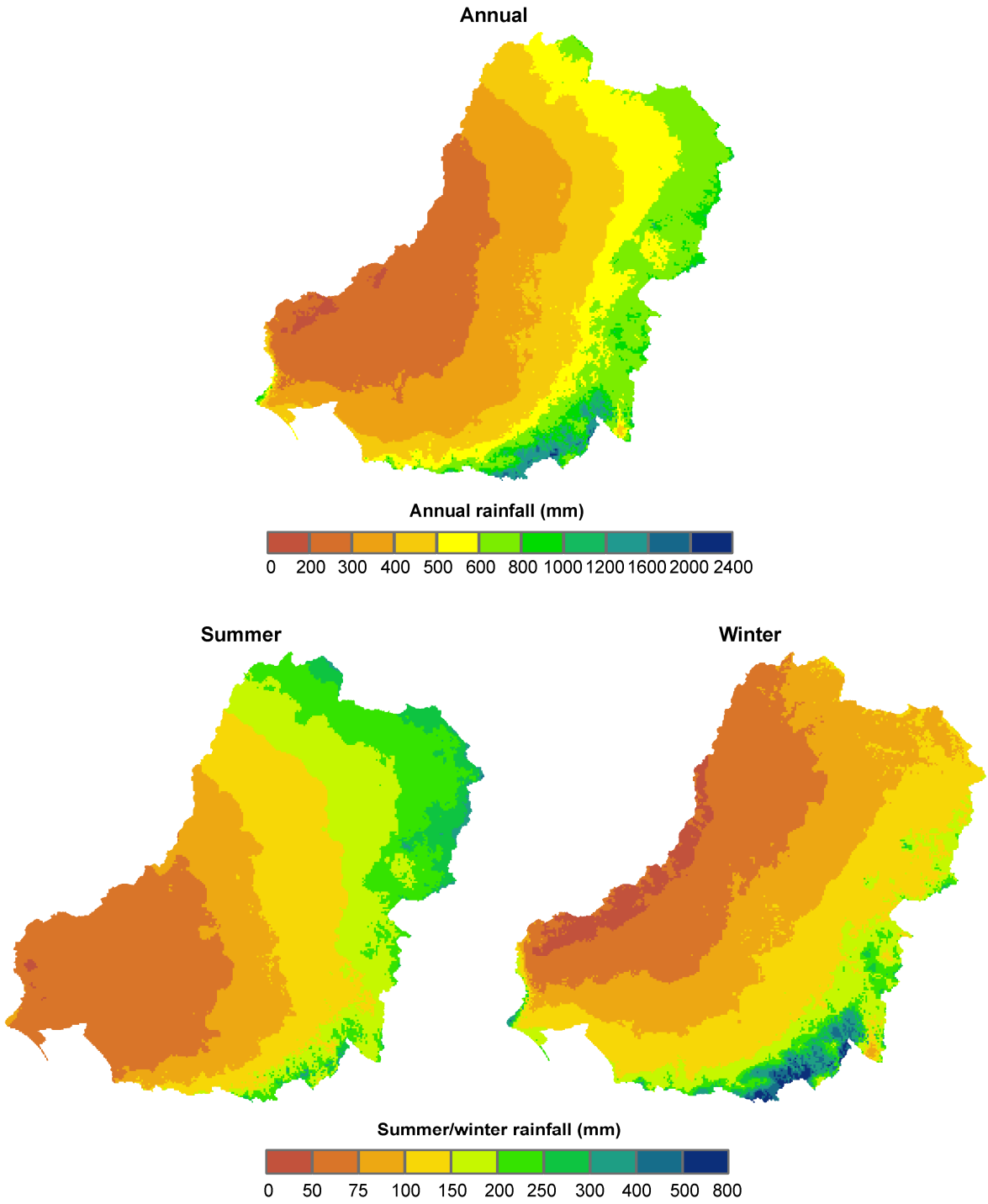

Figure 2-1. Mean rainfall: annual, summer (DJF) and winter (JJA)

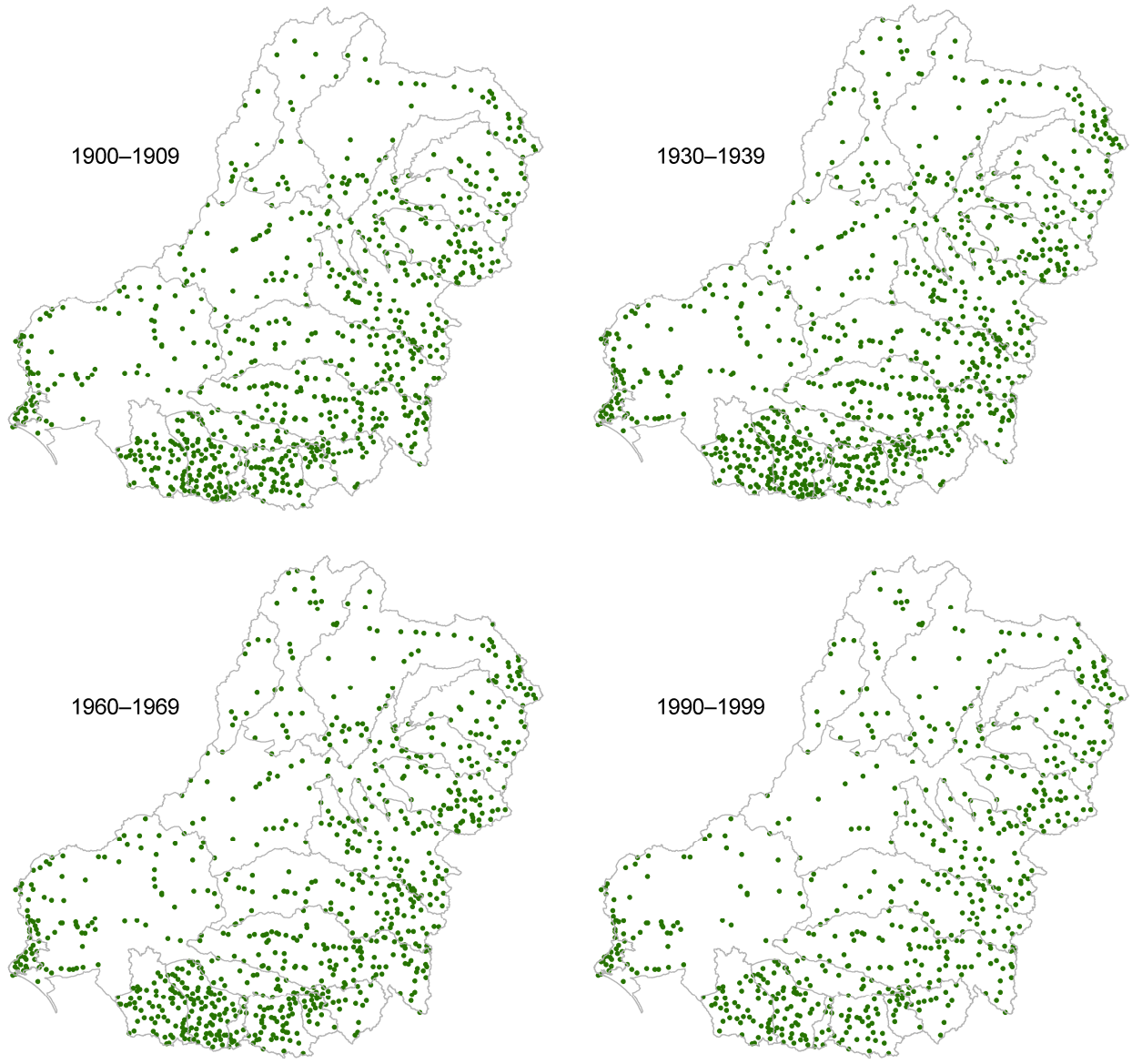

Figure 2-2. Locations of rainfall stations used to generate SILO Data Drill rainfall for various decades
(stations shown in the plots have more than 2000 daily recorded values over the decade, that is, more than 55 percent of the data)

2.3 Areal potential evapotranspiration

Daily rainfall and potential evapotranspiration (PET) are required as input data for the rainfall-runoff modelling. The daily areal potential evapotranspiration (APET) is calculated from 0.05^{o} x 0.05^{o} climate data from the SILO Data Drill (temperature; relative humidity, calculated as actual vapour pressure divided by saturation vapour pressure; and incoming solar radiation) using Morton's wet environment evapotranspiration algorithms (http://www.bom.gov.au/averages and Morton, 1983; Chiew and Leahy, 2003).

The APET is defined as the evapotranspiration that would take place, if there was unlimited water supply, from an area large enough that the effects of any upwind boundary transitions are negligible, and local variations are integrated to an areal average. The APET is therefore conceptually the upper limit to actual evapotranspiration in the rainfall-runoff modelling.

The rainfall-runoff modelling results are much less sensitive to errors in the PET data than they are to errors in the rainfall data. It is also easier to provide reliable PET data for the rainfall-runoff modelling, because compared to rainfall, PET is relatively conservative in space with little day-to-day variation.

Figures 2-3, 2-4, 2-5 and 2-6 show the mean annual, summer and winter air temperature, average relative humidity, incoming solar radiation and APET respectively across the MDB. The mean annual APET averaged across the MDB is 1443 mm, varying from 1700 mm in the north to 1000 mm in the south.

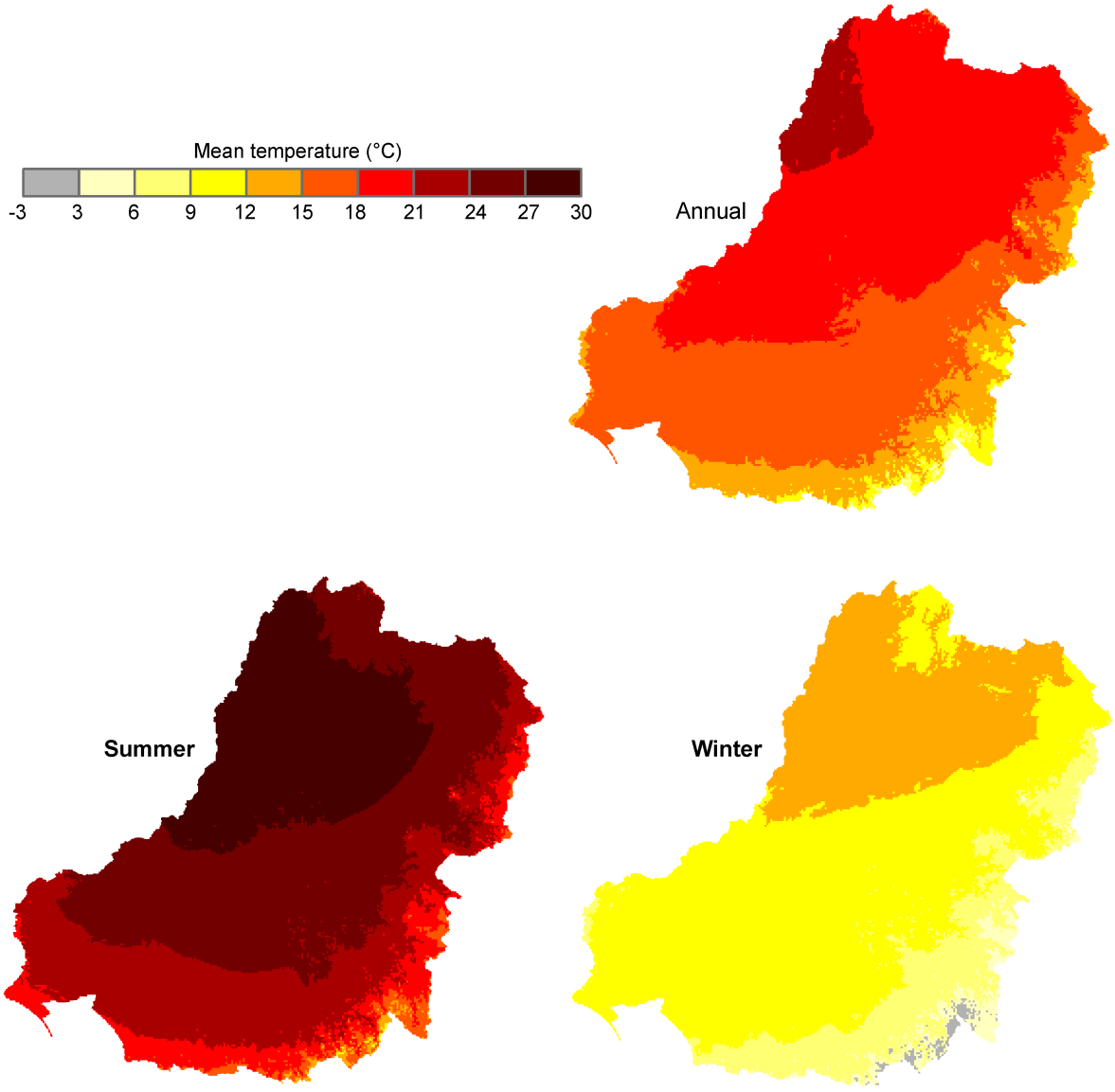

Figure 2-3. Mean temperature: annual, summer (DJF) and winter (JJA)

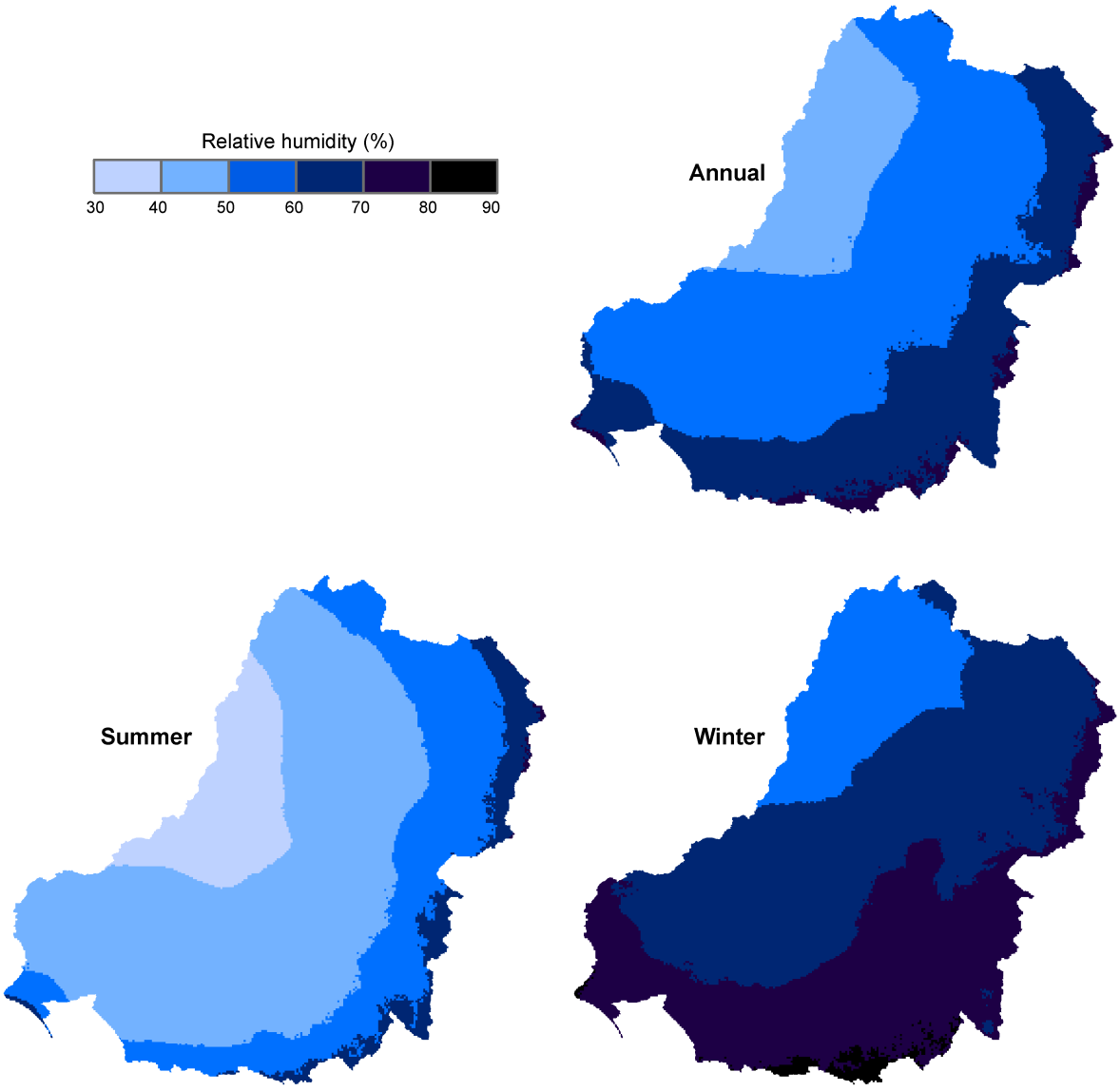

Figure 2-4. Mean relative humidity: annual, summer (DJF) and winter (JJA)

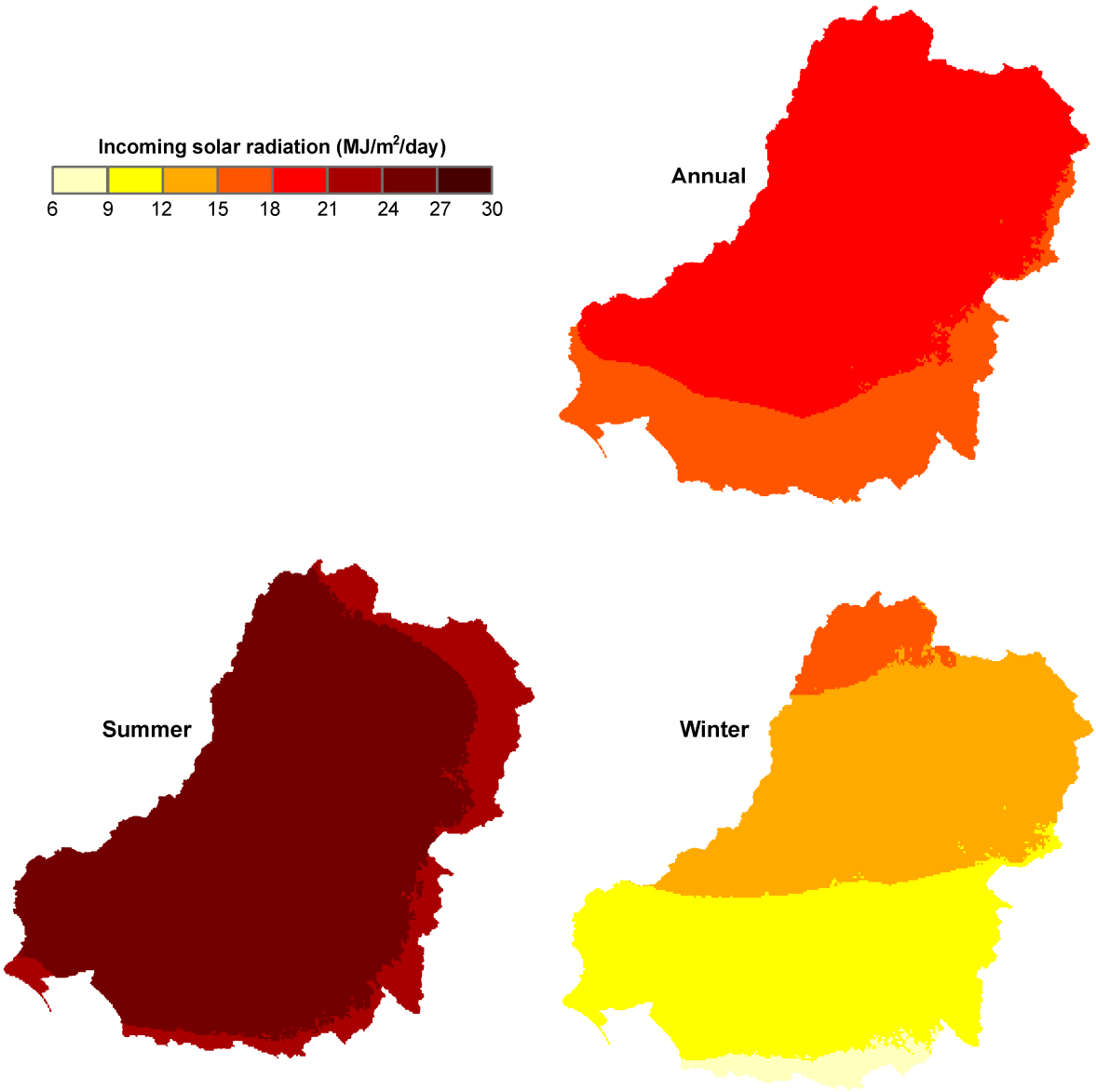

Figure 2-5. Mean incoming solar radiation: annual, summer (DJF) and winter (JJA)

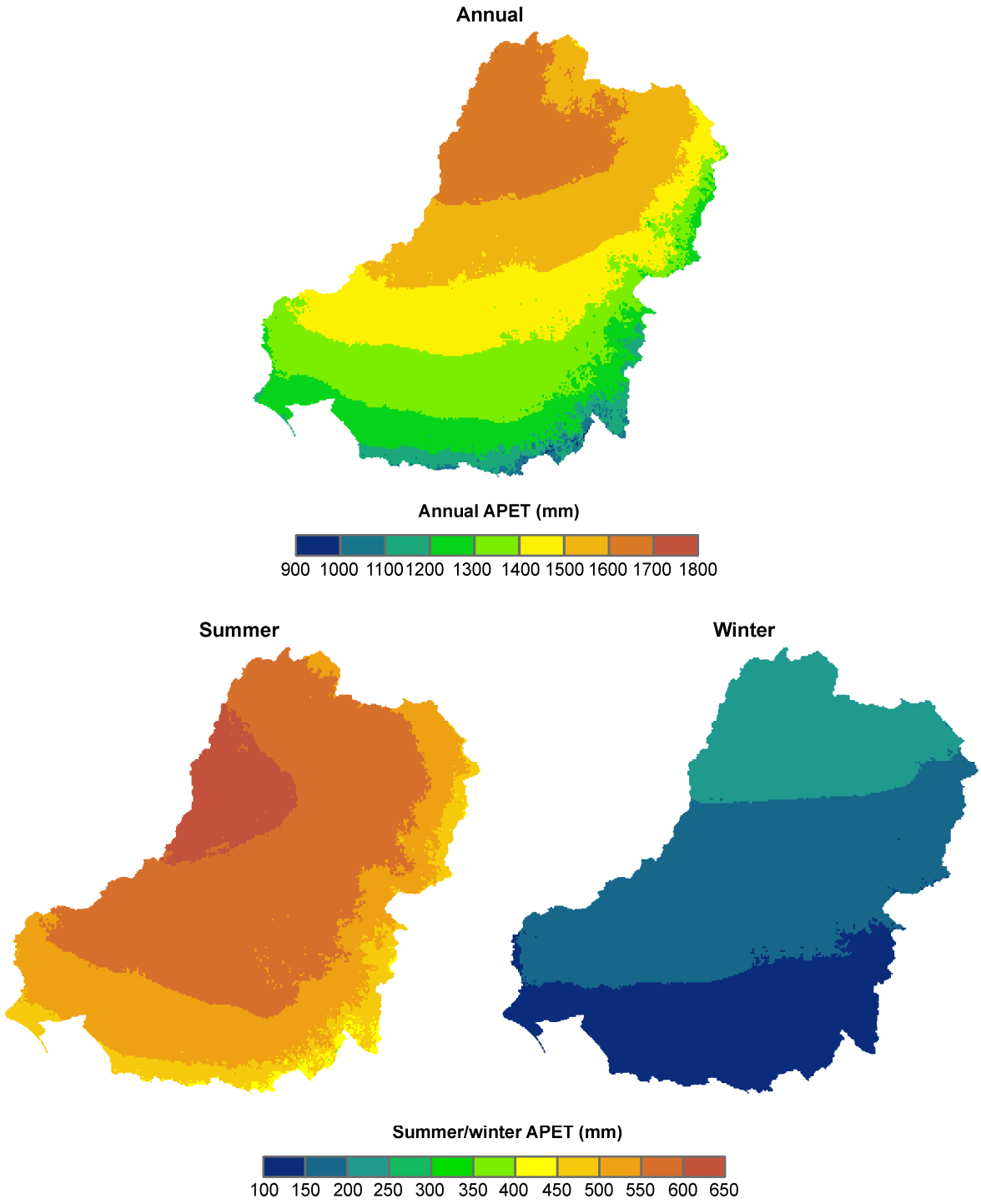

Figure 2-6. Mean areal potential evapotranspiration: annual, summer (DJF) and winter (JJA)

3 Recent climate data (Scenario B)

3.1 Method

The recent climate scenario (Scenario B) is used to assess future water availability should the climate in the future prove to be similar to that of the past ten years. The mean annual rainfall averaged over the Murray-Darling Basin (MDB) in the past ten years (1997 to 2006) is 440 mm, which is 4 percent lower than the 1895 to 2006 mean (457 mm). However, rainfall over the past ten years in the southern MDB is significantly lower than the long-term mean.

The Scenario B modelling is carried out only where the mean annual rainfall over the past ten years is statistically significantly different from the long-term mean. Figure 3-1 shows the difference between the 1997 to 2006 mean annual rainfall and the 1895 to 2006 long-term mean annual rainfall for the 18 MDB regions defined for this project. Regions are shown in red if the 1997 to 2006 mean annual rainfall is significantly different to the 1895 to 1996 rainfall, at a statistical significance level of $\alpha = 0.2$ with the Student-t and Rank Sum tests. The statistical significance depends on the difference between the 1997 to 2006 and 1895 to 1996 mean annual rainfalls and the inter-annual rainfall variability. The Scenario B modelling is therefore carried only for the Eastern Mount Lofty Ranges, Wimmera, Loddon-Avoca, Campaspe, Goulburn-Broken, Ovens, Murray and Murrumbidgee regions. Potter et al. (2008) present a detailed analysis and discussion of recent rainfall and runoff characteristics across the MDB relative to the long-term historical data.

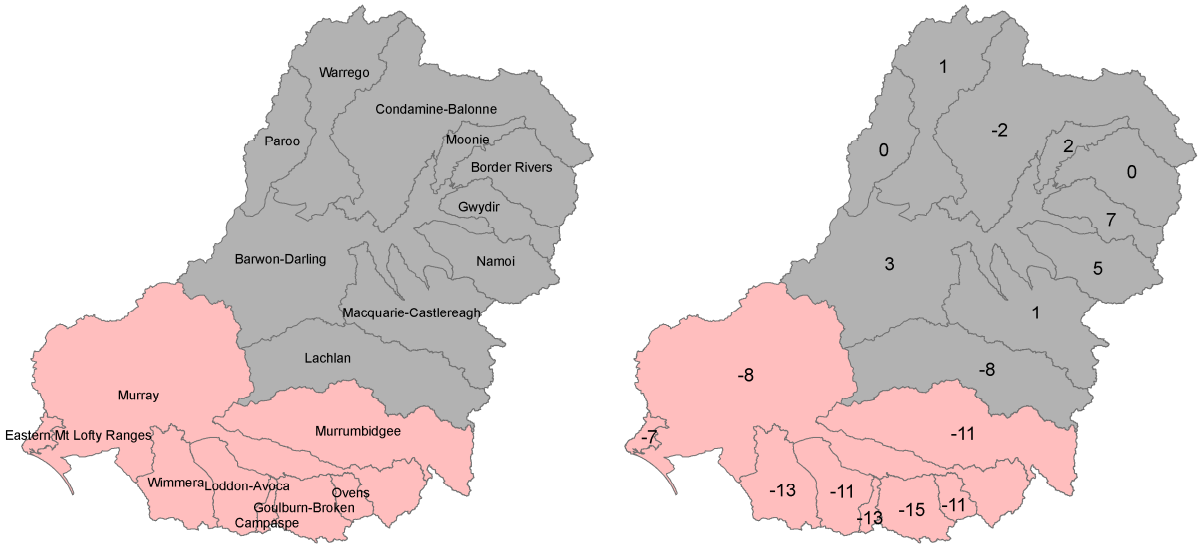

Figure 3-1. The 18 Murray-Darling Basin regions (left) and the percent difference between mean annual rainfall in 1997 to 2006 and in 1895 to 2006 (right) (regions are shown in red if the difference in mean annual rainfall is statistically significant)

Each region is considered separately in obtaining the Scenario B climate data. The first step in obtaining Scenario B climate data is generating 100 stochastic replicates of 112 years of single-site annual rainfall (averaged over the region). The annual rainfall series is generated based on the mean and standard deviation of 1997 to 2006 rainfall as well as other statistics of 1895 to 2006 rainfall. This annual rainfall modelling is described in Section 3.2. The second step is disaggregating the stochastically generated annual rainfall spatially and temporally to obtain daily rainfall and other climate data at 0.05^o x 0.05^o grids across the region. This disaggregation is described in Section 3.3.

The method therefore provides 100 stochastic replicates of 112 years of daily rainfall and other climate data at 0.05^o x 0.05^o grids across a region. The data are used to run the rainfall-runoff model. The river system and groundwater modelling use the stochastic replicate that produces a mean annual runoff for the region closest to the mean annual

runoff (not mean annual rainfall) in 1997 to 2006. The Scenario B data for the river system and groundwater modelling can therefore be different from those shown in Figure 3-1.

Detailed stochastic rainfall-runoff and river system modelling is carried out for the Gwydir region and the area encompassing the Loddon-Avoca, Campaspe and Goulburn-Broken regions (where the Goulburn Simulation Model is used for the river system modelling). In this detailed modelling, reported in Frost et al. (2008), all the stochastic replicates are used to explore how the range of plausible annual inflow sequences affects the modelling results. The method used to obtain the Scenario A, B and C stochastic climate data for the detailed stochastic hydrological modelling is the same as that described here.

3.2 Annual rainfall modelling

The single-site version of the lag-one autoregressive annual rainfall model of Frost et al. (2007) is used to generate the stochastic annual rainfall. The model allows for non-Gaussian rainfall distribution using Box-Cox transformation and considers parameter uncertainty using Bayesian methods with Markov Chain Monte Carlo parameter estimation.

The stochastic annual rainfall model has four parameters, μ, σ, ψ and λ, which relate to the mean, standard deviation, lag-one serial correlation and the Box-Cox transformation (related to skewness) respectively. The mean and standard deviation are estimated based on the 1997 to 2006 data, and the other two parameters are estimated based on the 1895 to 2006 data. The skewness and serial correlation are estimated using the entire data set because estimating the parameters using data from only the past ten years would lead to very large uncertainties in the estimates.

The ability of the stochastic model to reproduce the statistics of the historical data are verified by generating 50,000 replicates of 112-year annual rainfall data, and comparing the statistics of the stochastically generated data with those of the historical data. The results (Figure 3-2) indicate that the stochastic model can reproduce satisfactorily the various standard statistics (mean, standard deviation, skewness, minimum, maximum, ten-year rainfall sums and different lag serial correlations), with the statistics of the historical rainfall data falling between the 5^{th} and 95^{th} percentile values of the 50,000 stochastically generated replicates.

Figure 3-2 shows a selection of the verification statistics, stratified into the 1895 to 2006 and 1997 to 2006 periods, for the eight MDB regions where Scenario B modelling is carried out. The verification indicates that most statistics from most of the historical series lie within the 90 percent confidence limits of the 50,000 replicates from the stochastic rainfall model. Most of the observed values, particularly the mean and standard deviation, are close to the median values from the 50,000 replicates. The observed skewness for the 1997 to 2006 period are generally lower than the median values from the 50,000 replicates, but are mostly within the 90 percent confidence limits. The plots also highlight the wider confidence limits and therefore greater parameter uncertainties in the statistics estimated from ten years of data (1997–2006) compared to the statistics estimated from 112 years of data (1895–2006).

3.3 Disaggregation of annual rainfall

The 100 replicates of 112-year annual rainfall series (averaged over an entire region) are disaggregated spatially and temporally to obtain daily rainfall series for 0.05^{o} x 0.05^{o} grids across the region. This is undertaken for each year of the generated series by first selecting a ‘similar’ year in the historical record to that of the generated annual rainfall, and then disaggregating the generated annual rainfall spatially and temporally using the observed rainfall pattern from that ‘similar’ year (and scaling the rainfall such that the annual rainfall over the region is the same as the generated annual rainfall). For the other climate data, the data from the ‘similar’ year are used directly.

The modified method of fragments approach of Maheepala and Perera (1996) is used to determine the observed year used for disaggregation. This method chooses the ‘similar’ year based on two criteria: it has a similar annual rainfall as the stochastically generated annual rainfall; and the January rainfall for that year gives a realistic rainfall correlation from December (from the previous year which has already been obtained) to January.

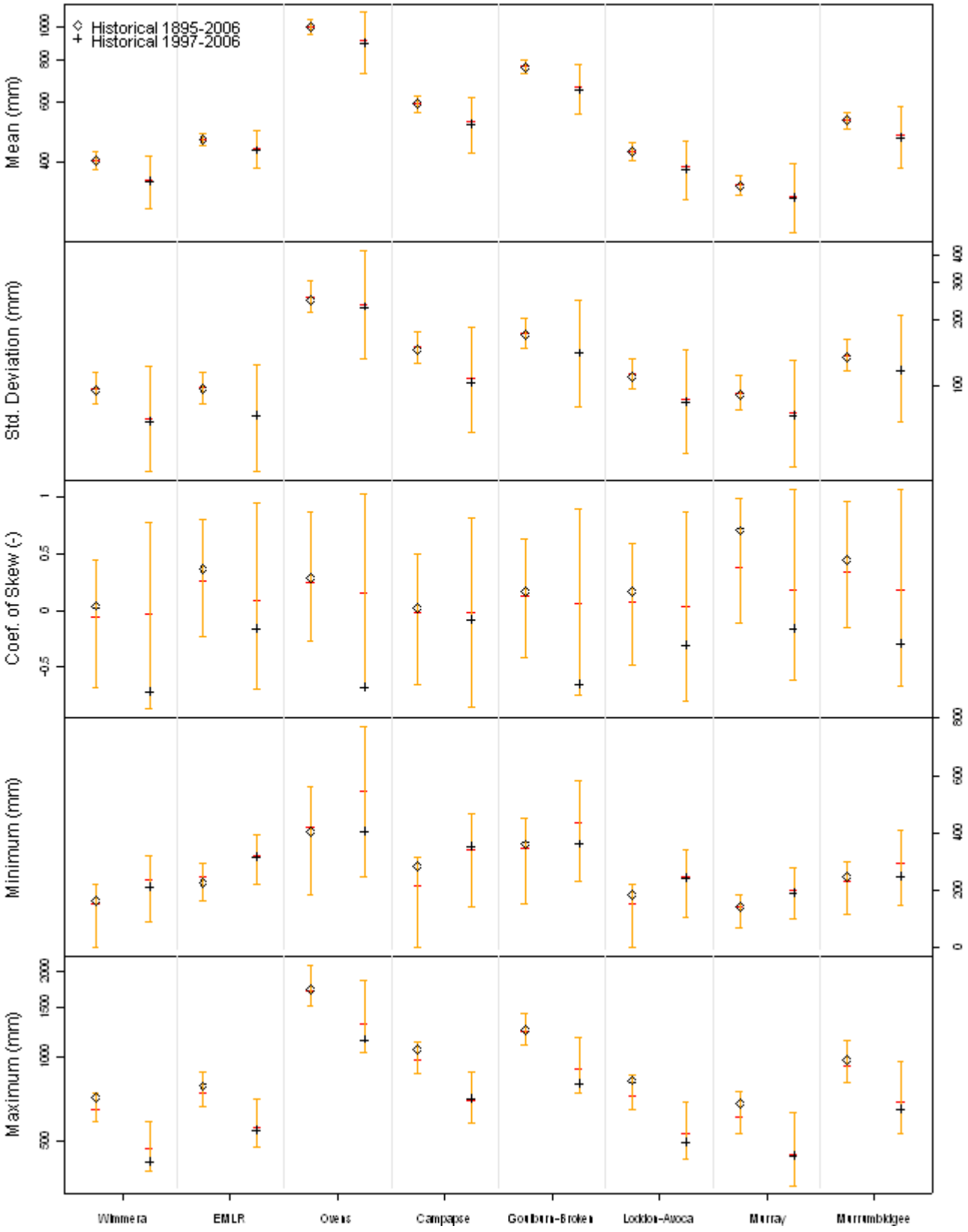

Figure 3-2. Comparison of statistics of the 50,000 112-year stochastic annual rainfall replicates with statistics of the historical data. Plots show the 5th percentile (lower yellow whisker), median (red line) and 95th percentile (upper yellow whisker) values from the 50,000 replicates and the values for the historical data.
For each region, the statistics on the left are for 1895–2006 and those on the right are for 1997–2006.

4 Future climate data (Scenario C)

4.1 Method

The future climate scenario (Scenario C) is used to assess the range of possible climate conditions around the year 2030. Forty-five future climate variants, each with 112 years of daily climate sequences for 0.05^{o} x 0.05^{o} grid cells across the Murray-Darling Basin (MDB), are used for the rainfall-runoff modelling. The future climate variants come from scaling the 1895 to 2006 climate data to represent the climate around 2030, based on analyses of 15 global climate models (GCMs) and three global warming scenarios.

The steps used to obtain the 45 112-year daily climate series are summarised below.

- Three global warming scenarios for ~2030 relative to ~1990 are used: high, medium and low. These three scenarios are inferred from the Fourth Assessment Report of the Intergovernmental Panel on Climate Change (IPCC AR4) (IPCC, 2007) and the latest climate change projections for Australia (CSIRO and Australian Bureau of Meteorology, 2007). This step is described in detail in Section 4.2.
- Archived monthly simulations from 15 IPCC AR4 GCMs are analysed to estimate the change in rainfall and other climate variables per degree of global warming. Each GCM is analysed separately. Data from each of the four seasons are also analysed separately. This step is described in detail in Section 4.3.
- The percent changes in the climate variables per degree of global warming for each of the four seasons from the 15 GCMs are then multiplied by the change in temperature for each of the three levels of global warming to obtain the 45 sets of 'seasonal scaling' factors. The seasonal scaling factors are then used to scale the historical daily climate data from 1895 to 2006 to obtain the 45 future climate variants, each with 112 years of daily climate data. The rainfall and other climate projections for ~2030 relative to ~1990 are presented in Section 4.4.
- The changes in the daily rainfall distribution are also considered by scaling the different rainfall amounts differently. This is described in detail in Section 4.5.

The method used here takes into account two types of uncertainties. The first uncertainty is in the global warming projection, due to the uncertainties associated with projecting greenhouse gas emissions and predicting how sensitive the global climate is to greenhouse gas concentrations. The second uncertainty is in GCM modelling of local climate in the MDB. The method also takes into account different changes in each of the four seasons as well as changes in the daily rainfall distribution. The consideration of changes in the daily rainfall distribution is important because many GCMs indicate that future extreme rainfall in an enhanced greenhouse climate is likely to be more intense, even in some regions where a decrease in mean seasonal or annual rainfall is projected. As high rainfall events generate large runoff, the use of simpler methods that assume the entire rainfall distribution to change in the same way would lead to an underestimation of total runoff.

There are simpler as well as more complex methods to obtain future catchment-scale climate data to drive hydrological models (see Chiew (2006a) for overview of methods). In particular, statistical and dynamic downscaling methods that relate large synoptic-scale atmospheric variables to catchment-scale rainfall can potentially provide more reliable future rainfall inputs to drive hydrological models. However, the use of downscaling methods was not possible given the time constraints of this project. The downscaling methods also may not necessarily provide more reliable future rainfall than the method used in this project because: (i) downscaling research is still developing and has not been used for hydrologic investigations of this scale; (ii) it is difficult to calibrate the downscaling method for a large region like the MDB; and (iii) there are limited archived daily GCM simulations from which to downscale to provide the range of uncertainties in the future climate.

The method used here is similar to, but not the same as, the approach used by CSIRO and Australian Bureau of Meteorology (2007) (http://www.climatechangeinaustralia.gov.au) to provide the climate change projections for Australia. The key differences are: (i) this project uses 15 of the 23 IPCC AR4 GCMs, while the CSIRO/BoM projections use all 23 GCMs; (ii) this project assesses the extreme range of global warming by ~2030; and (iii) this project also considers changes in the daily rainfall distribution.

As the future climate series (Scenario C) is obtained by scaling the historical daily climate series from 1895 to 2006 (Scenario A), the daily climate series for Scenarios A and C have the same length of data (112 years) and the same sequence of daily climate (for example, potential changes in the frequency and timing of daily rainfall are not considered). Scenario C is therefore not a forecast climate at 2030, but a 112-year daily climate series based on 1895 to 2006 data for projected global temperatures at ~2030 relative to ~1990.

4.2 Global warming

This section summarises the global warming projections leading to the three global warming scenarios used for this project. A comprehensive picture of the present state of knowledge on global climate change can be found in the IPCC AR4 (IPCC, 2007; http://www.ipcc.ch). The recently released CSIRO and Australian Bureau of Meteorology (2007) report provides detailed future projections of Australian climate and discusses past climate characteristics and drivers of Australian climate.

There is an increasing body of research that supports a picture of a warming world with significant changes in regional climate systems. Eleven of the last 12 years rank among the 12 warmest years in the instrumental record of global surface temperature (since 1850) and the linear warming trend over the last 50 years is about 0.13^{o}C per decade (IPCC, 2007). However, since 1976, the global temperature has risen more sharply at 0.18^{o}C per decade (WMO, 2006). The global average temperature over the last 150 years is shown in Figure 4-1. Based on many lines of evidence including the widespread warming of the atmosphere and ocean, together with ice mass loss, the IPCC (2007) concluded that most of the observed increase in the global average temperature since the mid-20th century is very likely due to the observed increase in anthropogenic greenhouse gas concentrations.

The global climate system is highly complex, and therefore it is inappropriate to simply extrapolate past trends to predict future conditions. To estimate future climate change, scientists have developed emission scenarios for greenhouse gases and aerosols. The greenhouse gas emissions considered here are those due to human activities, such as energy generation, transport, agriculture, land clearing, industrial processes and waste. To provide a basis for estimating future climate change, the IPCC (2000) Special Report on Emission Scenarios (SRES) prepared 40 greenhouse gas and sulphate aerosol emission scenarios for the 21st century that combine a variety of assumptions about demographic, economic and technological factors likely to influence future emissions. Each scenario represents a variation within one of four ‘storylines’ (A1, A2, B1 and B2, see Table 4-1) with projected carbon dioxide, methane, nitrous oxide and sulphate aerosol emissions associated with each of the scenarios.

Increasing concentrations of greenhouse gases affect the radiative balance of the Earth. The balance between incoming solar radiation and outgoing heat radiation defines the Earth’s radiative budget and average temperature. Radiative forcing is the term given to an externally imposed change in the radiation balance, such as changes in atmospheric concentrations of greenhouse gases. Carbon dioxide dominates the radiative forcing and has a warming effect.

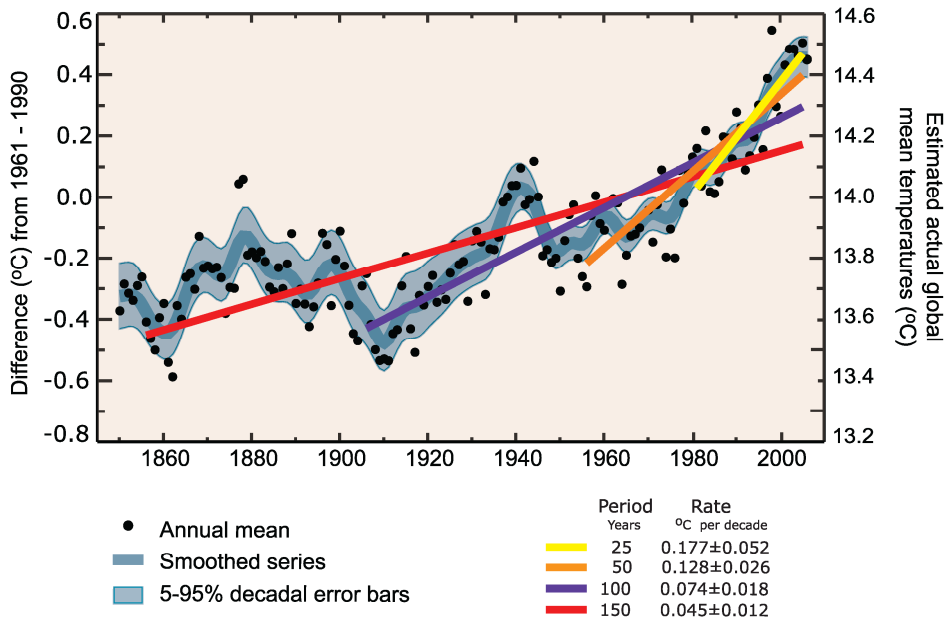

Figure 4-1. Global average temperature over the last 150 years (from IPCC, 2007)

Table 4-1. Storylines from the Intergovernmental Panel on Climate Change (2000) Special Report on Emission Scenarios

A1. The A1 storyline describes a future world of very rapid economic growth, a global population that peaks in mid-century and declines thereafter, and the rapid introduction of new and more efficient technologies. Major underlying themes are convergence among regions, capacity building and increased cultural and social interactions, with a substantial reduction in regional differences in per capita income. The A1 story line develops into three scenario groups that describe alternative directions of technological change in the energy system. They are distinguished by their technological emphasis: fossil intensive (A1FI), non fossil energy sources and technologies (A1T), or a balance across all sources (A1B) (where balanced is defined as not relying too heavily on one particular energy source, on the assumption that similar improvement rates apply to all energy supply and end use technologies).

A2. The A2 storyline describes a very heterogeneous world. The underlying theme is self reliance and preservation of local identities. Fertility patterns across regions converge very slowly, which results in continuously increasing population. Economic development is primarily regionally oriented and per capita economic growth and technological change more fragmented and slower than other storylines.

B1. The B1 storyline describes a convergent world with the same global population, that peaks in mid-century and declines thereafter, as in the A1 storyline, but with rapid change in economic structures toward a service and information economy, with reductions in material intensity and the introduction of clean and resource efficient technologies. The emphasis is on global solutions to economic, social and environmental sustainability, including improved equity, but without additional climate initiatives.

B2. The B2 storyline describes a world in which the emphasis is on local solutions to economic, social and environmental sustainability. It is a world with continuously increasing global population, at a rate lower than A2, intermediate levels of economic development, and less rapid and more diverse technological change than in the B1 and A1 storylines. While the scenario is also oriented towards environmental protection and social equity, it focuses on local and regional levels.

An illustrative scenario was chosen for each of the six scenario groups A1B, A1FI, A1T, A2, B1 and B2. All were considered equally sound by the IPCC.

The SRES scenarios do not include additional climate initiatives, which means that no scenarios are included that explicitly assume implementation of the United Nations Framework Convention on Climate Change or the emissions targets of the Kyoto Protocol.

The IPCC AR4 Working Group 1 Summary for Policymakers (IPCC, 2007) provides estimates of global warming for the year 2100 for six emission scenarios (B1, A1T, B2, A1B, A2 and A1F). The range of warming is based on 23 GCMs and results from a hierarchy of independent models and observational constraints. Important uncertainties, including the possibility of significant further amplification of climate change due to carbon cycle feedbacks, are also considered. The lower end of the warming range corresponds to the mean warming minus 40 percent, while the upper end of the range is the mean warming plus 60 percent. The range of global warming by 2100 is 1.1 to 6.4 ^{o}C.

Equivalent global warming values for 2030 are not provided by the IPCC (2007). The values required for this project and for broader Australian projections have been derived in a way that is consistent with the approach used by IPCC (2007) for 2100. The result is three predictions of the temperature change by ~2030 relative to ~1990: a low global warming of 0.45^{o}C (low end of SRES B1), medium global warming of 1.03^{o}C (average of the low and high global warming scenarios), and high global warming of 1.60^{o}C (high end of SRES A1T). These values are taken from Table 4.3 of the CSIRO and Australian Bureau of Meteorology (2007) study.

4.3 Change in climate variables per degree global warming

Global warming will lead to changes in regional climate. GCMs are the best tools available for simulating global and regional climate systems. There have been rapid improvements in climate modelling over the last few decades and the results from GCMs have been compared to a wealth of observational data. However, although GCMs have reasonable skill in simulating past climate and therefore providing some confidence in their use for climate projections, the range of future climate predictions from different GCMs is often large.

To account for the uncertainty in GCM simulation of future climate across the MDB, archived results from 15 of the 23 IPCC AR4 GCMs are used in this project. The GCM data are obtained from the Program for Climate Model Diagnosis and Intercomparison (PCMDI) website (http://www-pcmdi.llnl.gov). This project uses data from only 15 of the 23 GCMs because Scenario C future climate series were required to run the hydrological models in June 2007, and at that time only 15 GCMs were analysed and readily available. These 15 GCMs also have readily available daily rainfall data. In comparison, the CSIRO and Bureau of Meteorology (2007) climate change projections for Australia released in October 2007 used data from all 23 GCMs. The CSIRO and Bureau of Meteorology study also used weights to favour the use of GCMs that best reproduce the observed historical climate (rainfall, temperature and sea level pressure) across Australia. The weights in the CSIRO and Bureau of Meteorology study vary from 0.3 to 0.7, with the weights of the 15 GCMs used in this project all being above 0.5.

The 15 GCMs used are listed in Table 4-2. Monthly rainfall and other climate data are available for these GCMs for the period 1870 to 2100. For each GCM, and for each season and each GCM grid point, the simulated rainfall (or other climate variable) is plotted against simulated global average temperature. A linear regression is fitted through the data points and the slope of the linear regression gives the change in rainfall (or other climate variable) per degree of global warming (see Figure 4-2). The absolute change in the climate variable per degree of global warming is converted to a percent change per degree global warming relative to the model baseline climate of 1975 to 2005 (except in the case of temperature where the absolute value is used). In particular, the percent change is used for rainfall to reduce the effect of errors in the baseline climate on the magnitude of the simulated change (Whetton et al., 2005). One of the advantages of this method is that it decouples the model's response from the particular emission scenario used in the simulation, and the resultant change per degree global warming can be rescaled by the global warming values for any scenario.

Combinations of results from many runs for the same GCM are used (generally all A1B simulations for rainfall and temperature, and a combination of A1B and A2 runs for the other climate variables) to estimate the change in the climate variable per degree global warming. Relative humidity and incoming solar radiation data are not available for seven GCMs and are instead obtained from another GCM which matches the change in temperature most closely for each of these seven GCMs.

Table 4-2. List of 15 global climate models used

Global climate model	Modelling group, Country	Horizontal resolution (km)
CCCMA T47	Canadian Climate Centre, Canada	~250
CCCMA T63	Canadian Climate Centre, Canada	~175
CNRM	Meteo-France, France	~175
CSIRO-MK3.0	CSIRO, Australia	~175
GFDL 2.0	Geophysical Fluid, Dynamics Lab, USA	~200
GISS-AOM	NASA/Goddard Institute for Space Studies, USA	~300
IAP	LASG/Institute of Atmospheric Physics, China	~300
INMCM	Institute of Numerical Mathematics, Russia	~400
IPSL	Institut Pierre Simon Laplace, France	~275
MIROC-M	Centre for Climate Research, Japan	~250
MIUB	Meteorological Institute of the University of Bonn, Germany Meteorological Research Institute of KMA, Korea	~400
MPI-ECHAM5	Max Planck Institute for Meteorology DKRZ, Germany	~175
MRI	Meteorological Research Institute, Japan	~250
NCAR-CCSM	National Center for Atmospheric Research, USA	~125
NCAR-PCM1	National Center for Atmospheric Research, USA	~250

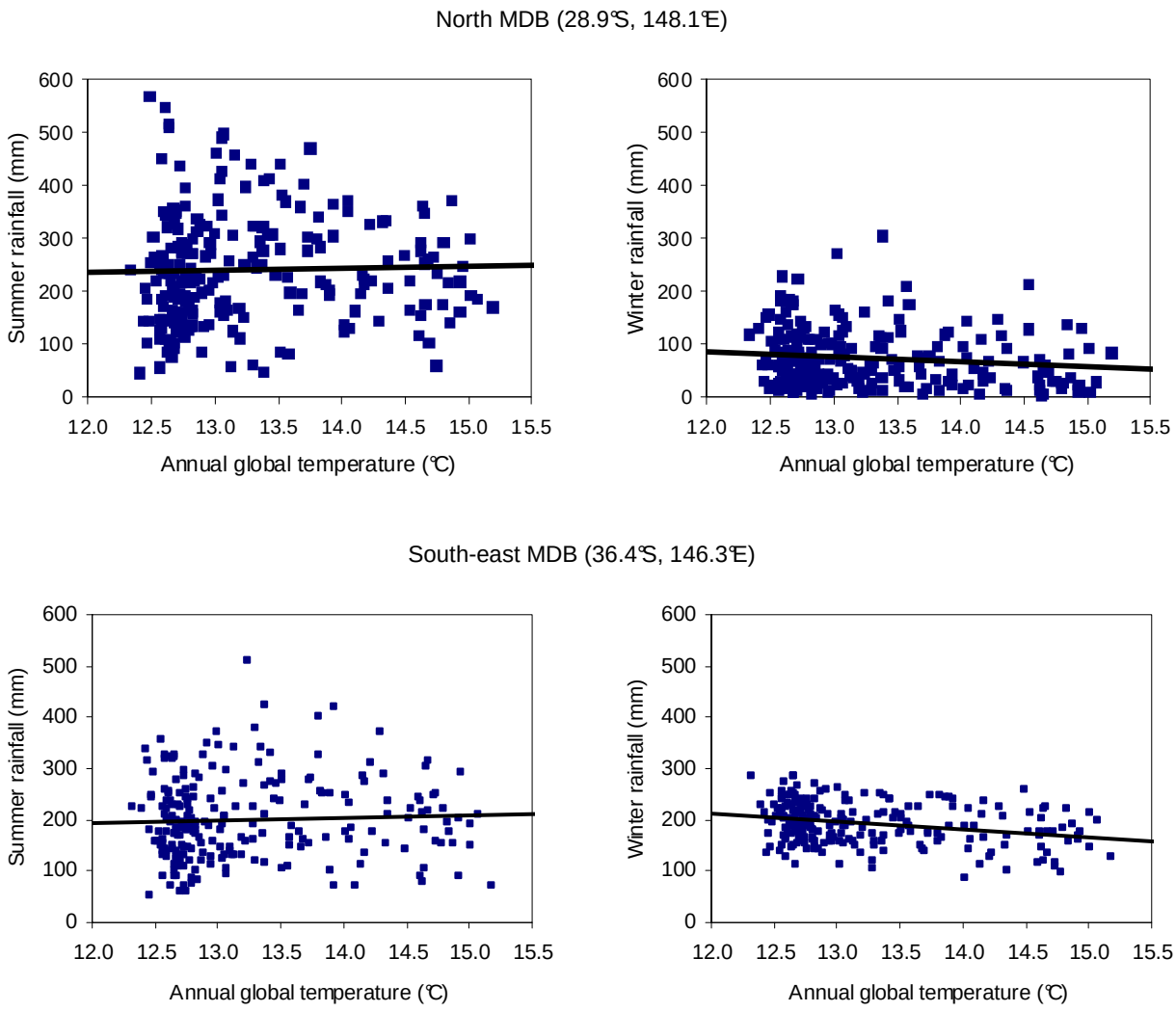

Figure 4-2. Example plots showing method used to estimate change in rainfall per degree global warming
(Plots show summer (DJF) and winter (JJA) rainfall versus global average temperature from CSIRO-MK3.0 GCM simulations for 1895 to 2100 for two selected GCM grids in the MDB, with the slope of the regression line giving the rainfall change per degree global warming)

4.4 Climate change projections for ~2030

The percent changes in the climate variables per degree global warming for each of the four seasons for the 15 GCMs from Section 4.3 are multiplied by the change in temperature for each of the three global warming scenarios in Section 4.2 to obtain the 45 sets of 'seasonal scaling' factors. The seasonal scaling factors are then used to scale the historical daily climate data from 1895 to 2006 to obtain the 45 future climate variants, each with 112 years of daily climate data.

The climate inputs required to run the rainfall-runoff model are daily rainfall and areal potential evapotranspiration (APET). The climate data are also used for the river system and groundwater recharge modelling. Rainfall is the main driver of runoff, with a 1 percent change in mean annual rainfall generally amplified to a 2 to 3.5 percent change in mean annual runoff. A 1 percent increase in mean annual APET generally leads to a 0.5 to 0.8 percent decrease in mean annual runoff (Chiew, 2006b; Jones et al., 2006). These are very general rules of thumb, and the daily future climate series obtained here are used in the rainfall-runoff modelling to provide more accurate results (see Chiew et al., 2008).

Figures 4-3, 4-4, 4-5 and 4-6 show the percent change in mean annual temperature, relative humidity, incoming solar radiation and APET, respectively, for ~2030 relative to ~1990 from the 15 GCMs for the medium global warming scenario. There is much better agreement in the future temperature projections from the 15 GCMs compared to the rainfall projections. The projections for the medium global warming scenario generally show a temperature increase of 0.6 to 1.5 ^{o}C, with the northern MDB showing greater warming. The GCMs indicate that the change in relative humidity by ~2030 relative to ~1990 is generally less than 3 percent and that the change in incoming solar radiation is generally less than 1 percent.

The temperature, relative humidity and incoming solar radiation are not used directly for the rainfall-runoff modelling, but are used to calculate the APET series required to run the rainfall-runoff model. In the analyses here, the daily historical temperature series from 1895 to 2006 is first increased by the temperature change in Figure 4-3 and the relative humidity and incoming solar radiation are scaled by the changes in Figures 4-4 and 4-5, respectively, to generate 112 years of future (~2030) daily climate series. The future climate series is then used to calculate the future APET series using the evapotranspiration algorithms described in Section 2.3. The results indicate that the mean annual APET in ~2030 relative to ~1990 for the medium global warming scenario will increase by 2 to 4 percent (Figure 4-6).

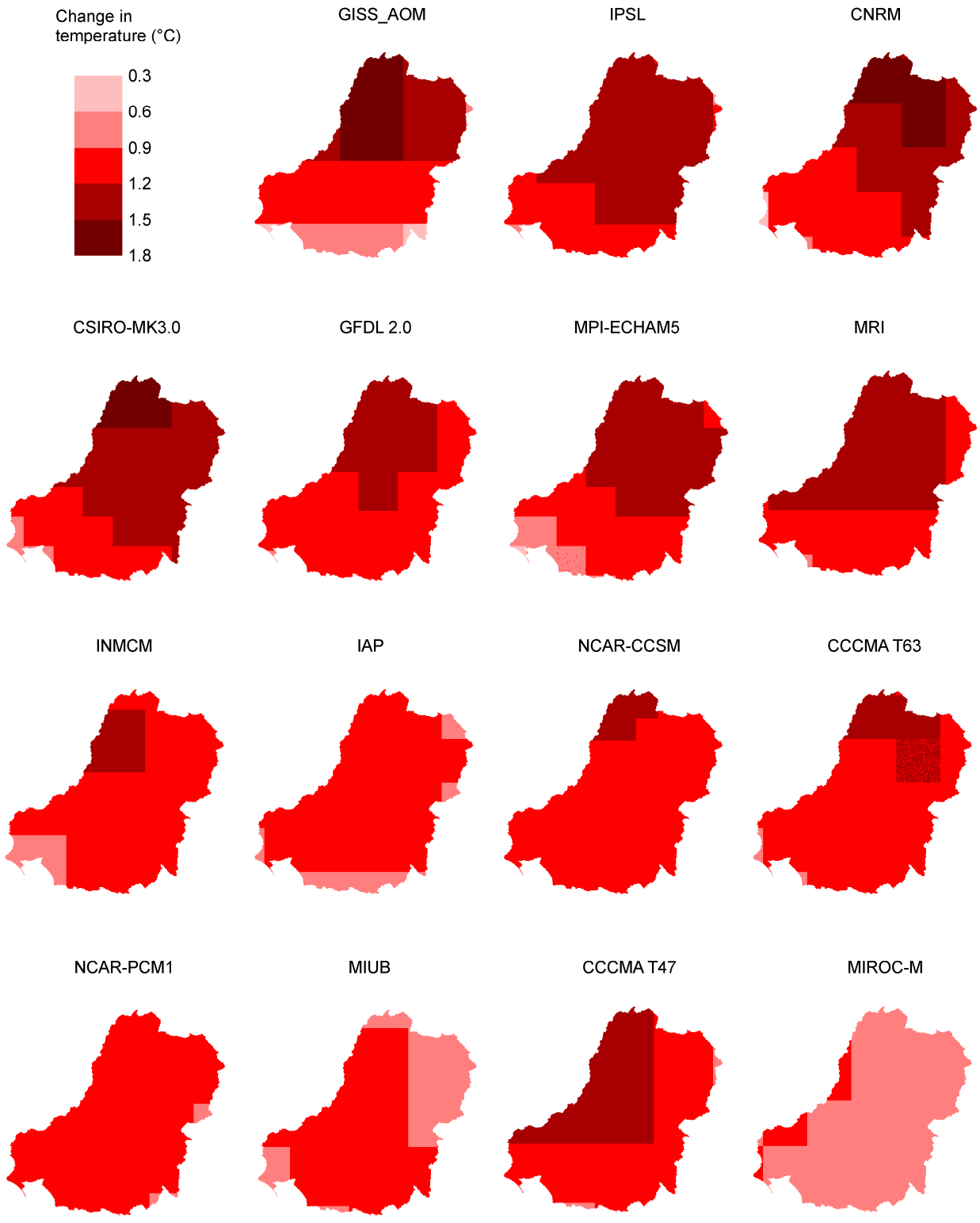

Figure 4-3. Percent change in mean annual temperature across the Murray-Darling Basin (~2030 relative to ~1990) from the 15 global climate models under the medium global warming scenario

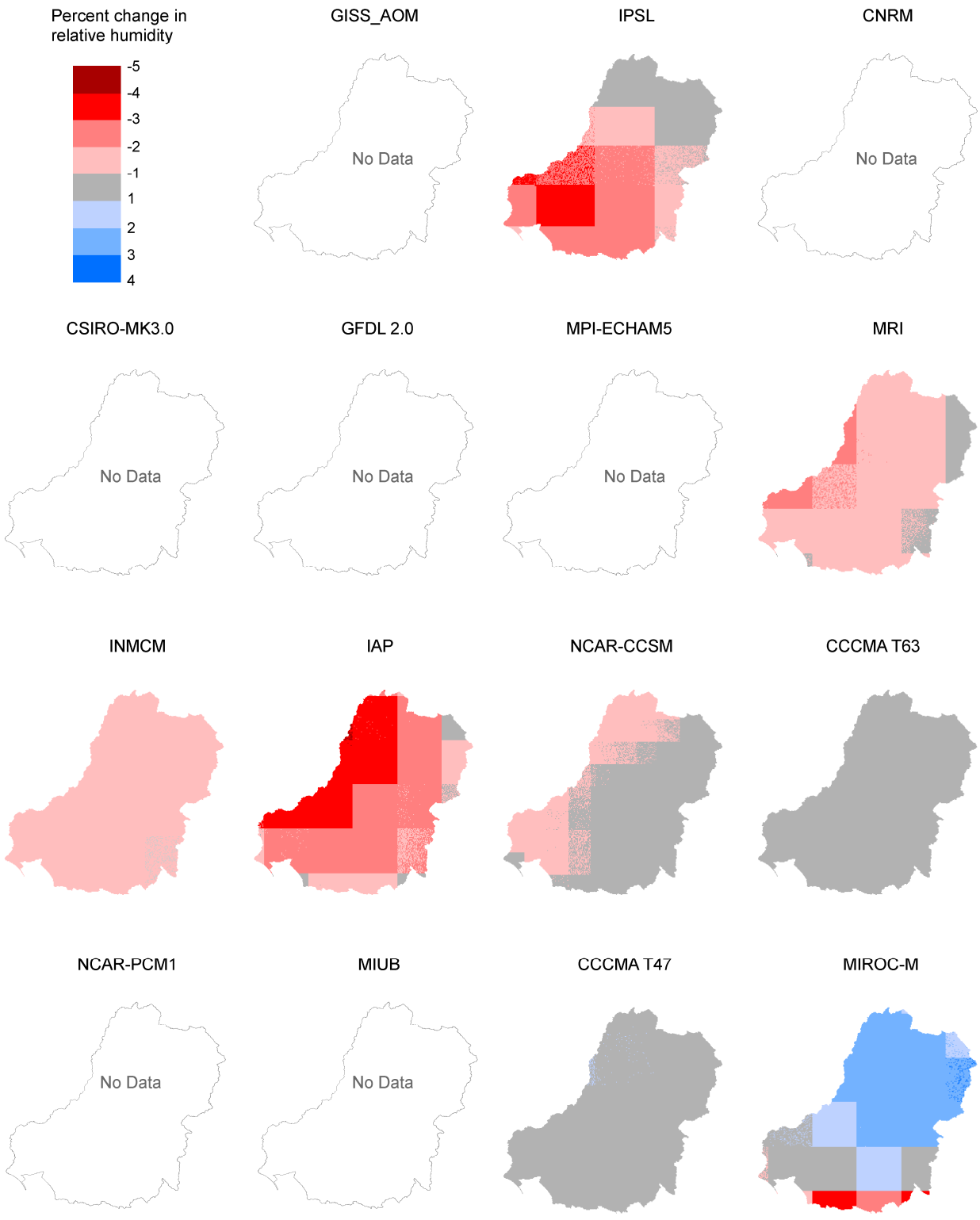

Figure 4-4. Percent change in mean annual relative humidity across the Murray-Darling Basin (~2030 relative to ~1990) from the 15 global climate models under the medium global warming scenario

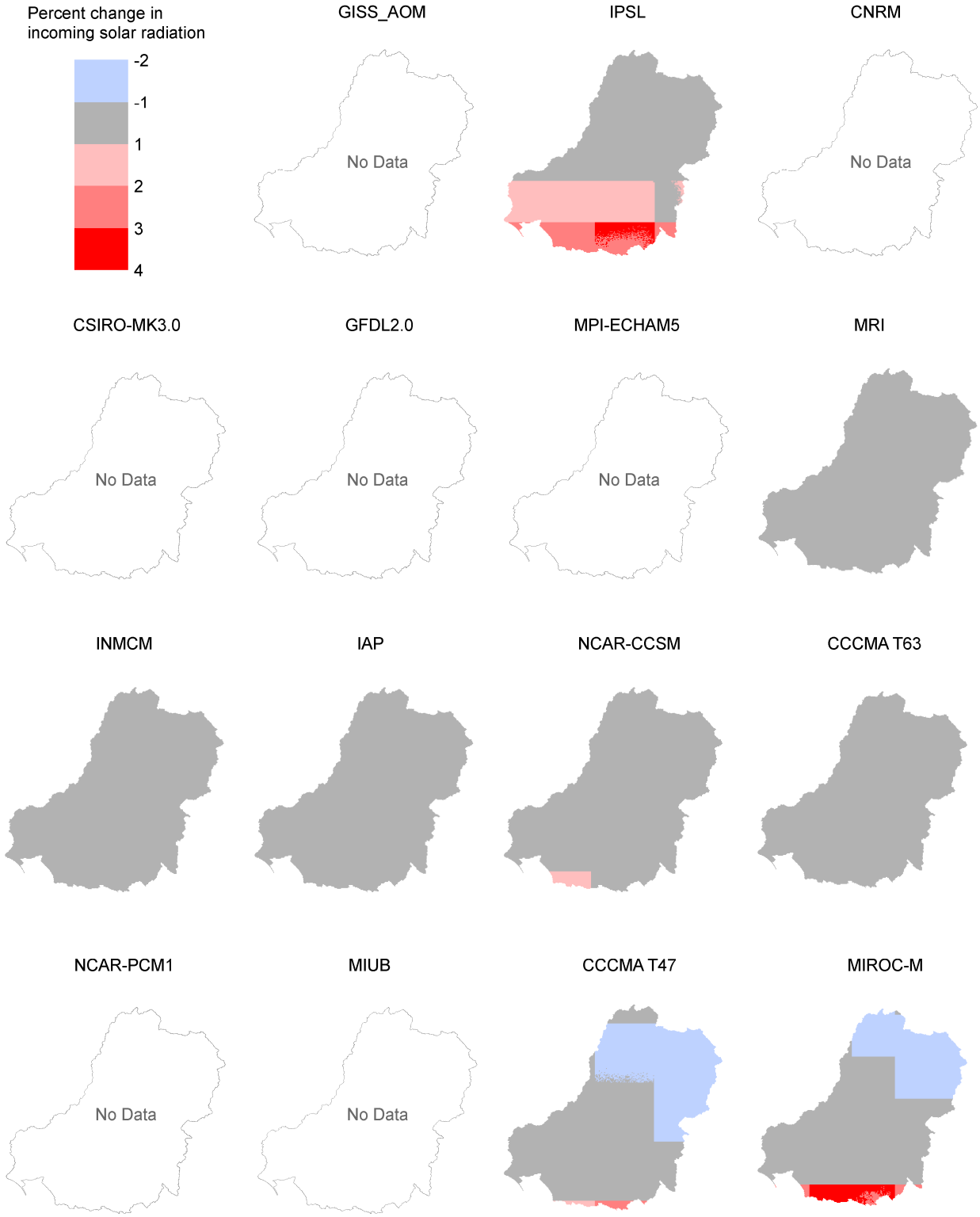

Figure 4-5. Percent change in mean annual incoming solar radiation across the Murray-Darling Basin (~2030 relative to ~1990) from the 15 global climate models under the medium global warming scenario

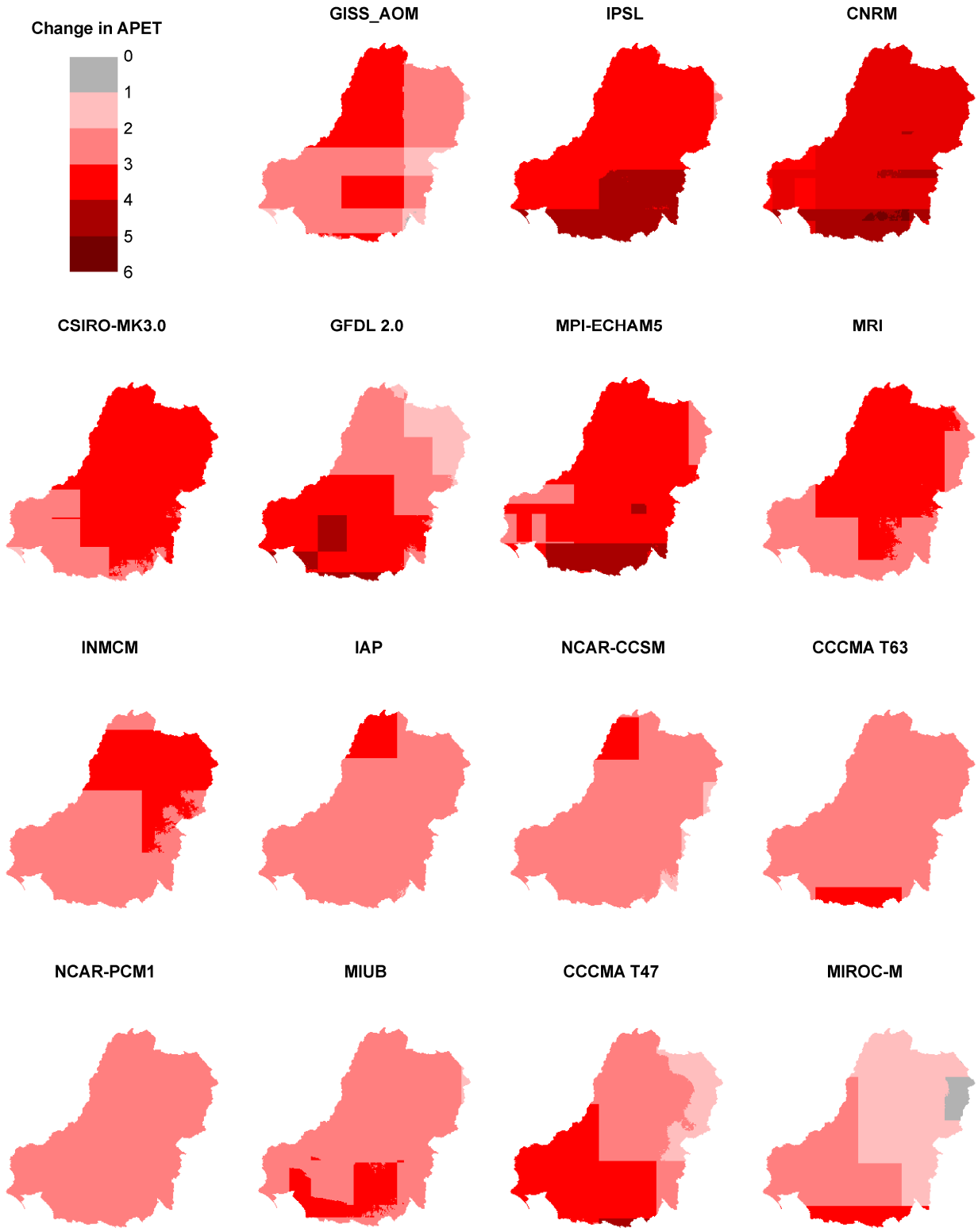

Figure 4-6. Percent change in mean annual areal potential evapotranspiration across the Murray-Darling Basin (~2030 relative to ~1990) from the 15 global climate models under the medium global warming scenario

Figures 4-7, 4-8 and 4-9 show the percent change in mean annual, summer, and winter rainfall, respectively, for ~2030 relative to ~1990 from the 15 GCMs for the medium global warming scenario. Figure 4-10 shows the number of GCMs that indicate a decrease in mean annual, summer, and winter rainfall. The results indicate that the potential changes in rainfall as a result of global warming can be very significant. However, there are considerable differences in the rainfall projections between GCMs, although the majority of GCMs shows a decrease in future mean annual rainfall. In the southern MDB, two-thirds to three-quarters of the GCMs show a decrease in mean annual rainfall. In the middle and northern parts of the MDB, one-half to two-thirds of the GCMs show a decrease in mean annual rainfall (Figures 4-7 and 4-10).

The majority of the GCMs indicate that future summer rainfall in the northern half of the MDB will increase, while similar numbers of GCMs show decreases and increases in summer rainfall in the southern half of the MDB (Figures 4-8 and 4-10). The GCM projections indicate that future winter rainfall is likely to be lower across the MDB, with almost all the GCMs showing less future winter rainfall in the southern half of the MDB, and more than two-thirds of the GCMs showing less winter rainfall in the northern half of the MDB (Figures 4-9 and 4-10).

As the seasonal scaling factors for the 45 future climate variants are obtained by multiplying the percent changes per degree global warming obtained from the 15 GCMs by the change in temperature for low, medium and high global warming, the driest and wettest variant will come from the high global warming scenario. The best estimate or median of the change in mean annual, summer, and winter rainfall and the extreme range of changes for the 0.05^{o} by 0.05^{o} grids across the MDB are shown in Figures 4-11, 4-12 and 4-13, respectively. The best estimate or median is defined as the median result from the 15 GCMs for the medium global warming scenario. The extreme dry estimate is defined as the second driest result from the high global warming scenario. The extreme wet estimate is defined as the second wettest result from the high global warming scenario. The second driest and second wettest results are used because they represent about the 10^{th} and 90^{th} percentile results. It should also be noted that the plots show results at 0.05^{o} grid cells, which are different to those used for the whole-of-region river system modelling reported in the regional reports from the Murray-Darling Basin Sustainable Yields Project. In the whole-of-region river system modelling, results from a single GCM (for each of the extreme dry, median and extreme wet) is used for each region, based on modelled mean annual runoff averaged over the region (see regional reports or Chiew et al., 2008).

The best estimate or median indicates that the future mean annual rainfall in the MDB in ~2030 relative to ~1990 will be lower, by about 2 percent in the north to 5 percent in the south. Averaged across the MDB, the best estimate or median is a 2.8 percent decrease in mean annual rainfall. There is considerable uncertainty in the projections, with the extreme dry and extreme wet estimates in the northern half of the MDB ranging from a 10 to 15 percent decrease to a 10 to 15 percent increase in mean annual rainfall. In the southern half of the MDB, the extreme estimates range from a 15 to 20 percent decrease in mean annual rainfall to a 5 to 10 percent increase in mean annual rainfall. In the southernmost MDB, the extreme estimates range from a decrease in mean annual rainfall of up to 20 percent to little change in mean annual rainfall (Figure 4-11). Averaged across the MDB, the extreme estimates range from a 13 percent decrease to an 8 percent increase in mean annual rainfall.

Figure 4-14 shows the mean monthly rainfall averaged over the 18 MDB regions defined for this project (see Figure 3-1 for the region locations), and the extreme range for the ~2030 climate. The extreme range is determined separately for each month from the high global warming scenario, with the second driest and the second wettest monthly result defining the lower bound and the upper bound, respectively.

In the northern regions, most of the rainfall occurs in the summer half of the year, and in the southernmost regions, most of the rainfall occurs in the winter half of the year. The plots also highlight the considerable differences between GCM projections, particularly in the northern regions. In the southernmost regions (Eastern Mount Lofty, Wimmera, Loddon-Avoca, Campaspe, Goulburn-Broken and Ovens), all the GCMs predict a decrease in rainfall in the winter half of the year when most of the rainfall and runoff occurs.

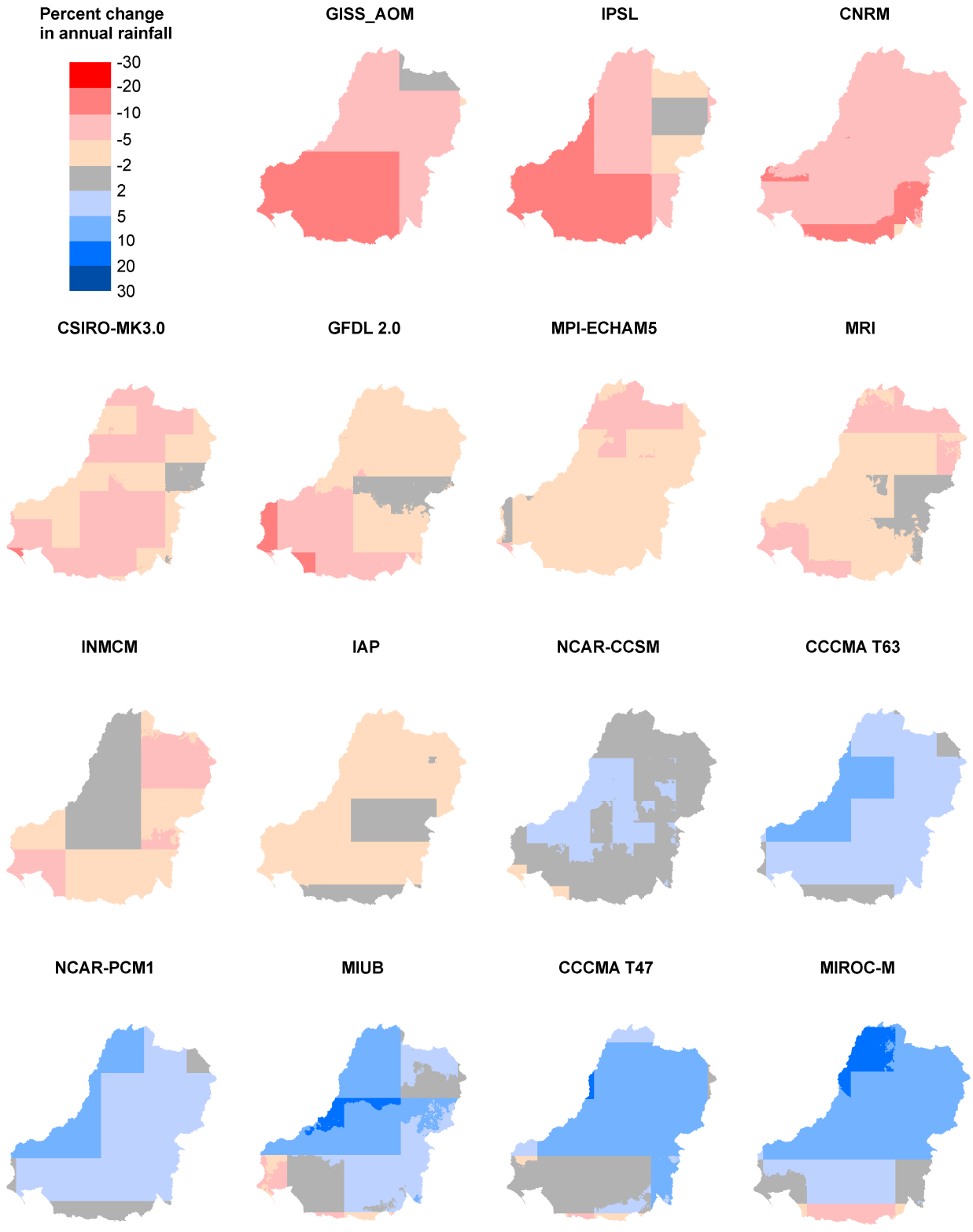

Figure 4-7. Percent change in mean annual rainfall across the Murray-Darling Basin (~2030 relative to ~1990) from the 15 global climate models under the medium global warming scenario

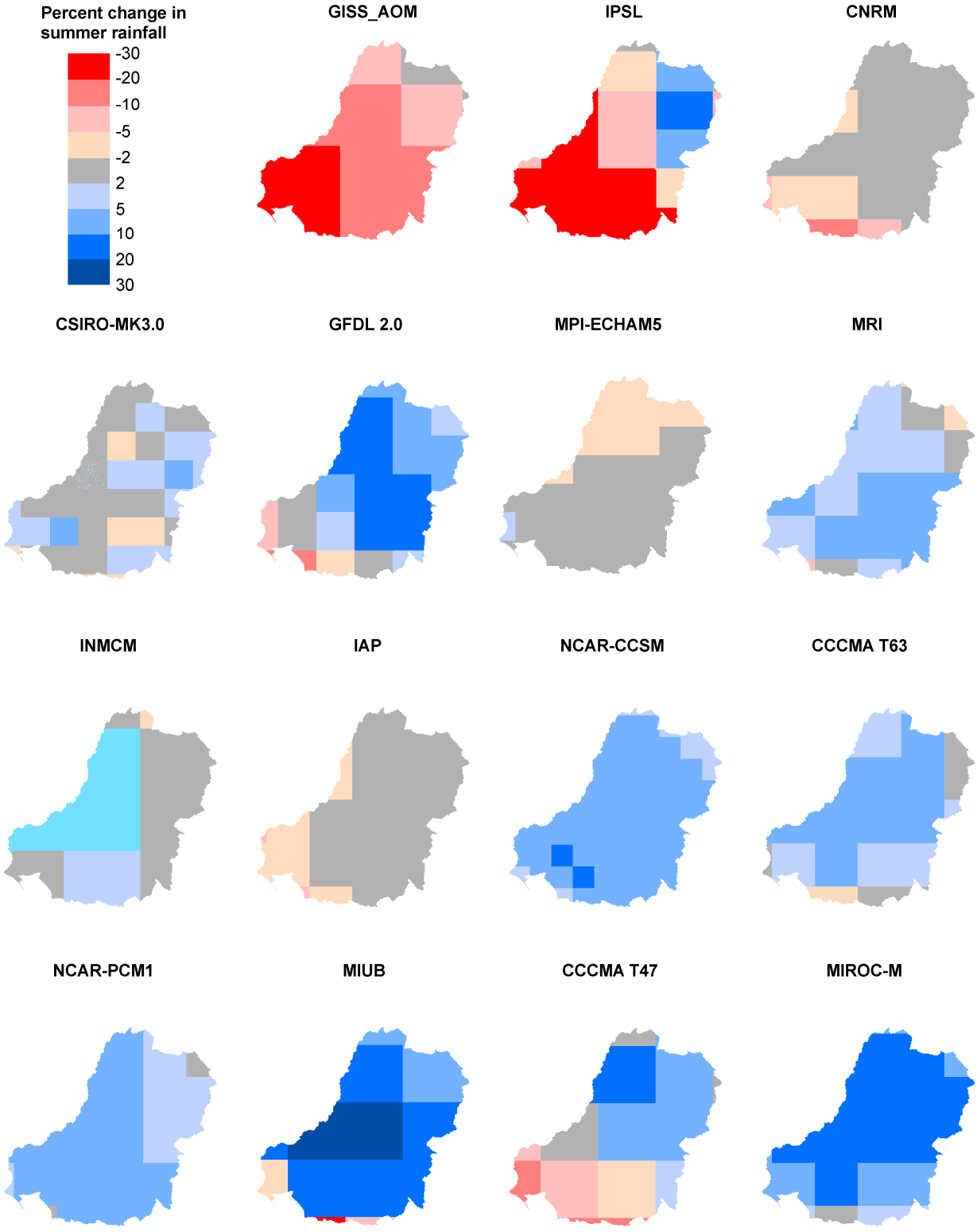

Figure 4-8. Percent change in mean summer (DJF) rainfall across the Murray-Darling Basin (~2030 relative to ~1990) from the 15 global climate models under the medium global warming scenario

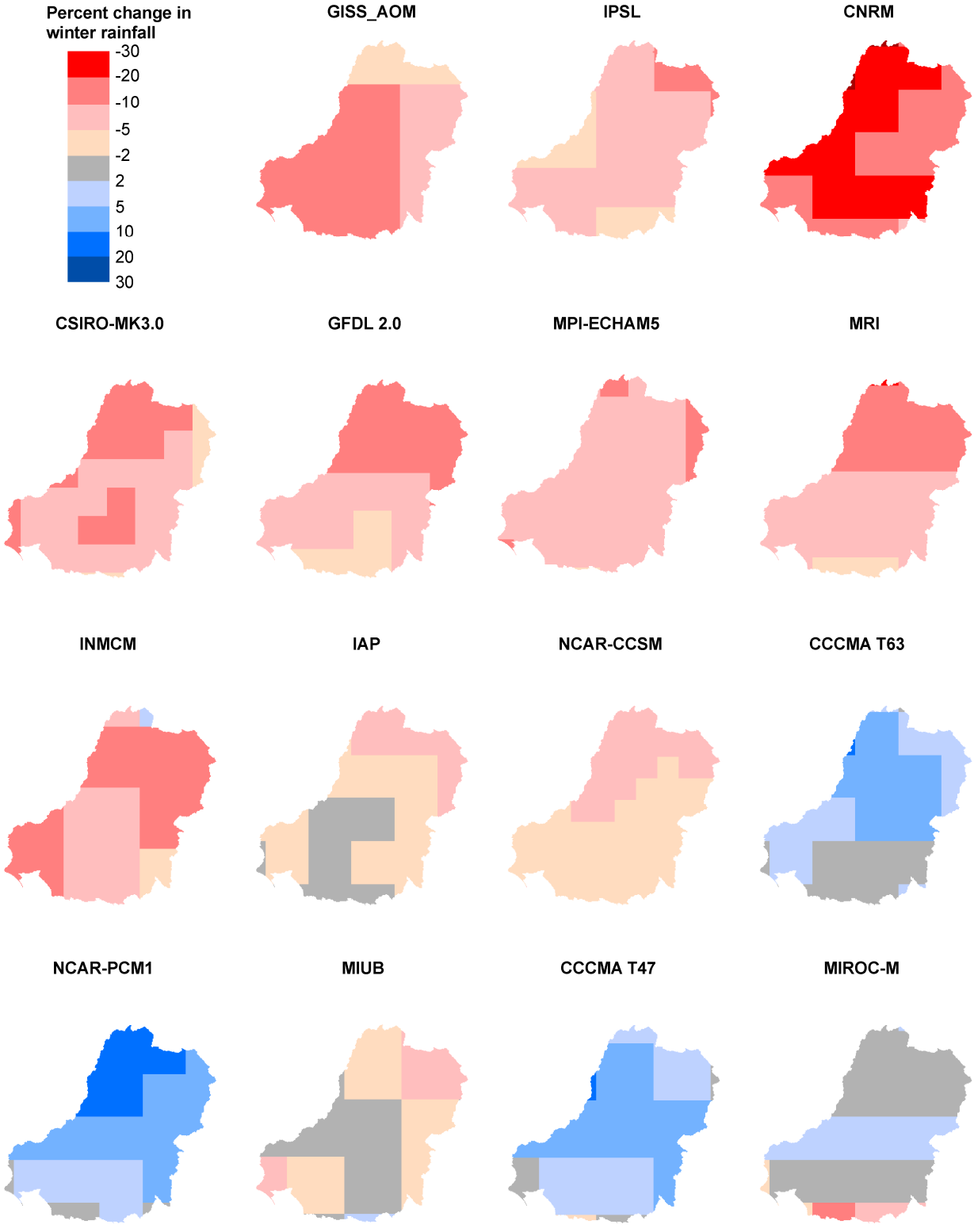

Figure 4-9. Percent change in mean winter (JJA) rainfall across the Murray-Darling Basin (~2030 relative to ~1990) from the 15 global climate models under the medium global warming scenario

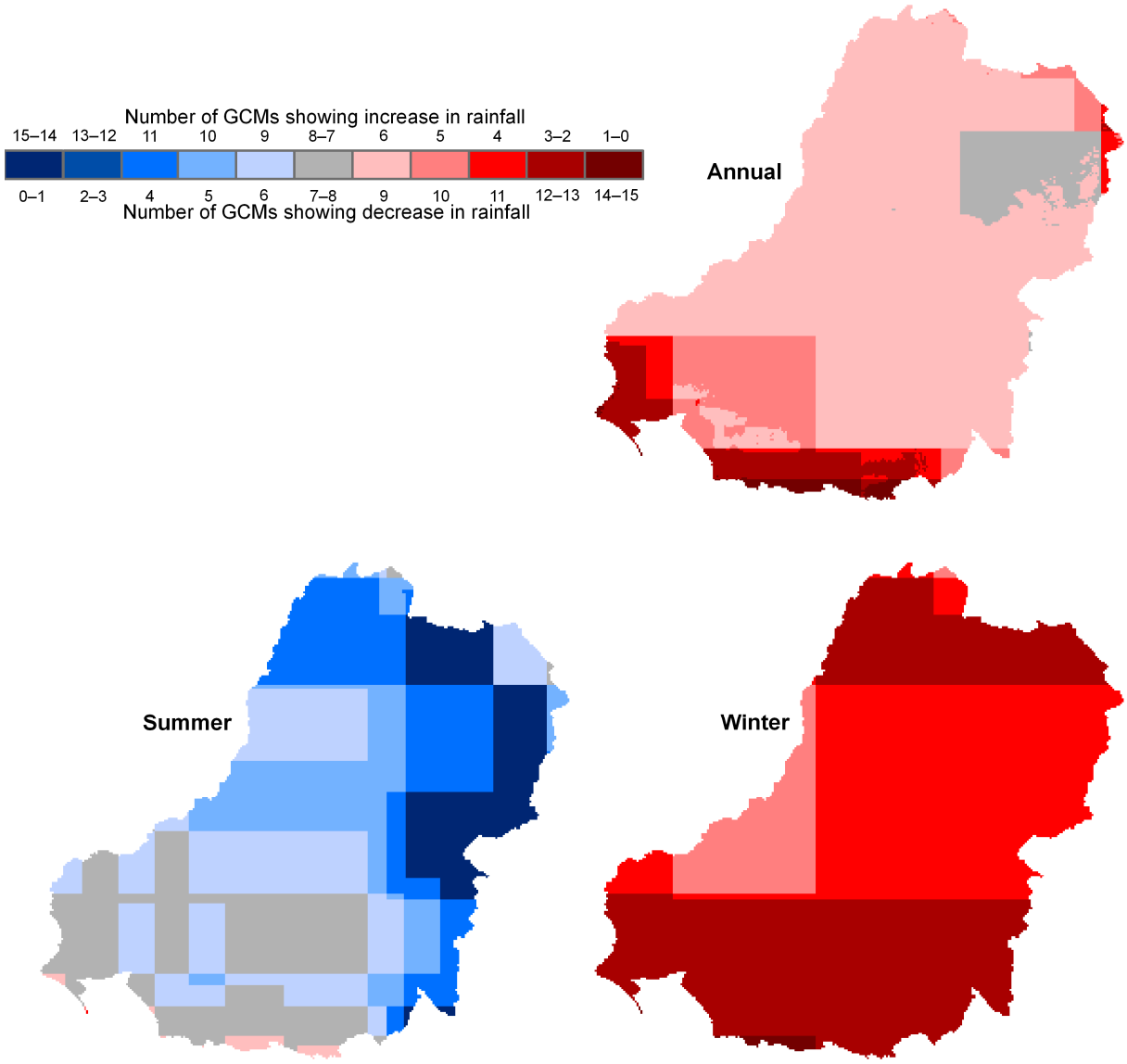

Figure 4-10. Number of global climate models showing a decrease (or increase) in future mean annual, summer (DJF), and winter (JJA) rainfall (note that 15 global climate models are used)

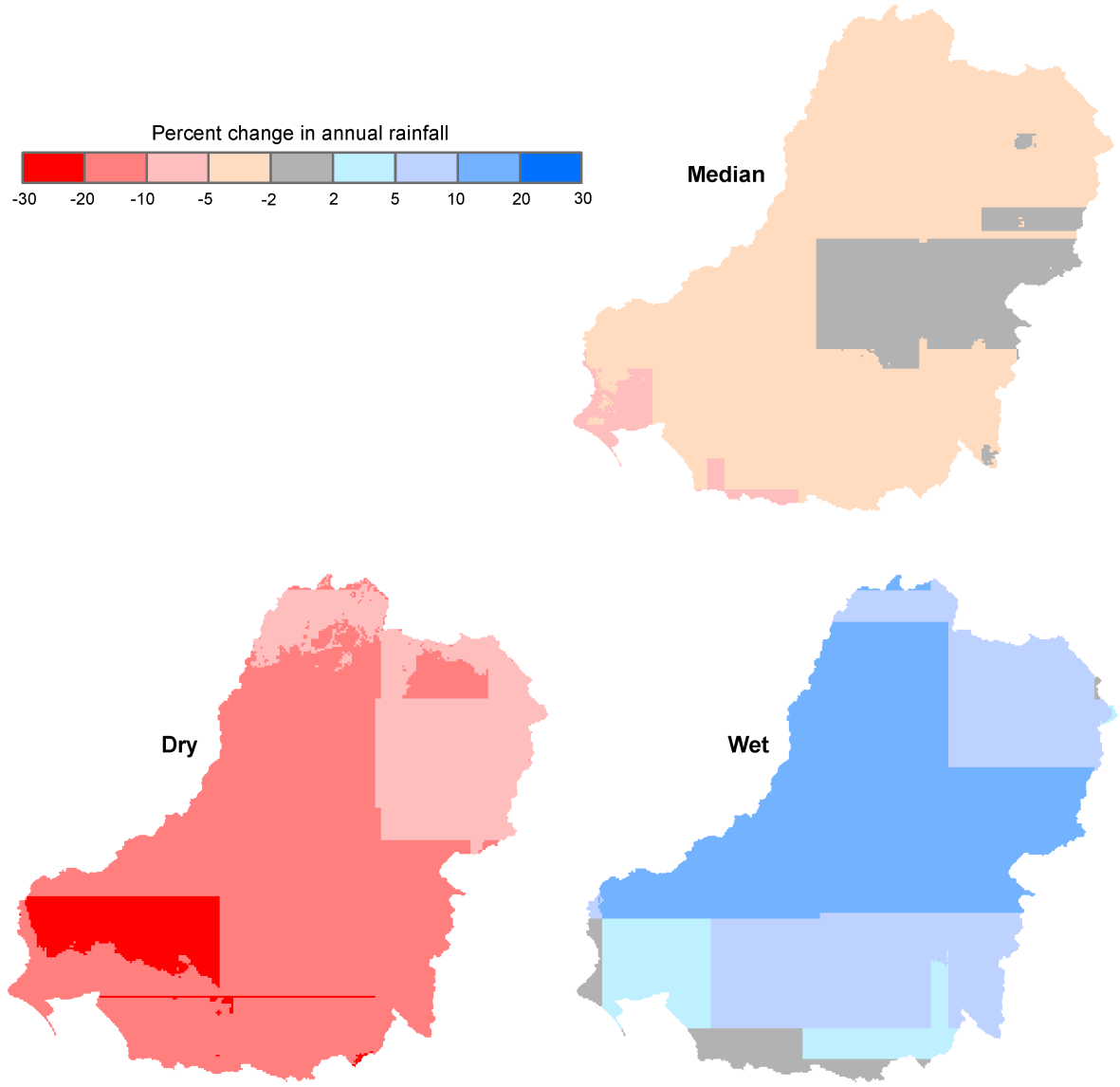

Figure 4-11. Percent change in mean annual rainfall across the Murray-Darling Basin (~2030 relative to ~1990) for the best estimate or median and the extreme dry and extreme wet variants

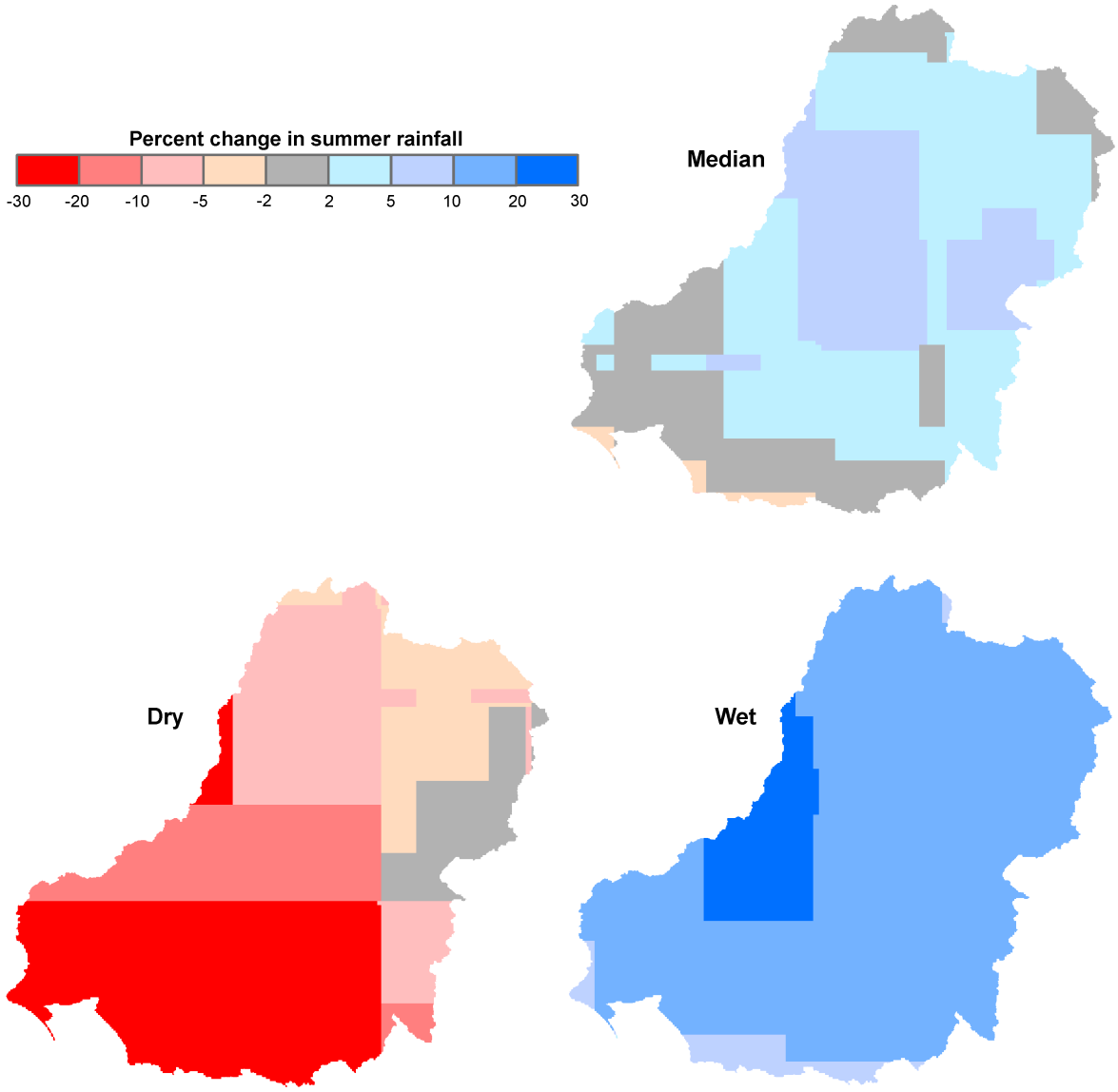

Figure 4-12. Percent change in mean summer (DJF) rainfall across the Murray-Darling Basin (~2030 relative to ~1990) for the best estimate or median and the extreme dry and extreme wet variants

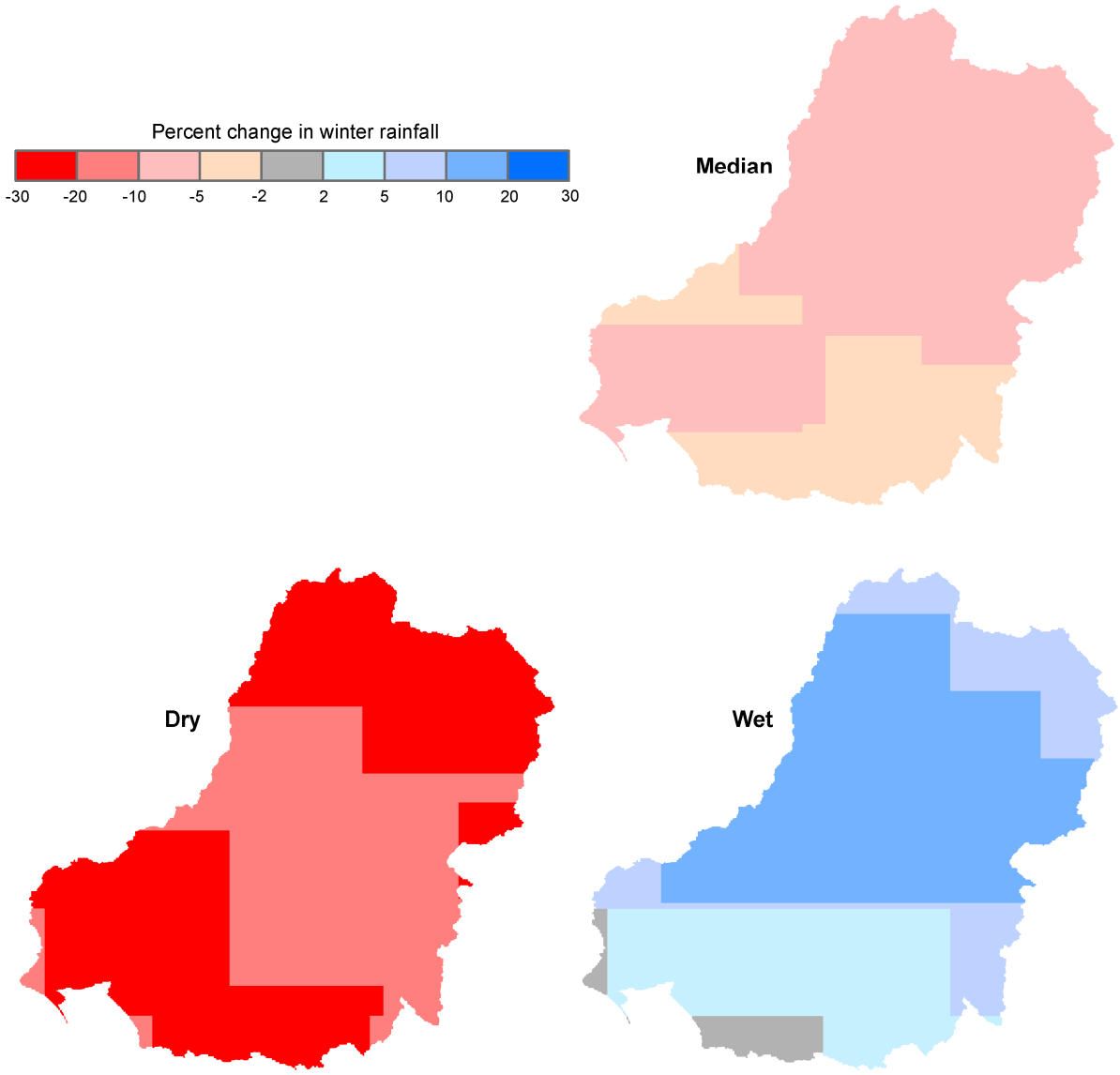

Figure 4-13. Percent change in mean winter (JJA) rainfall across the Murray-Darling Basin (~2030 relative to ~1990) for the best estimate or median and the extreme dry and extreme wet variants

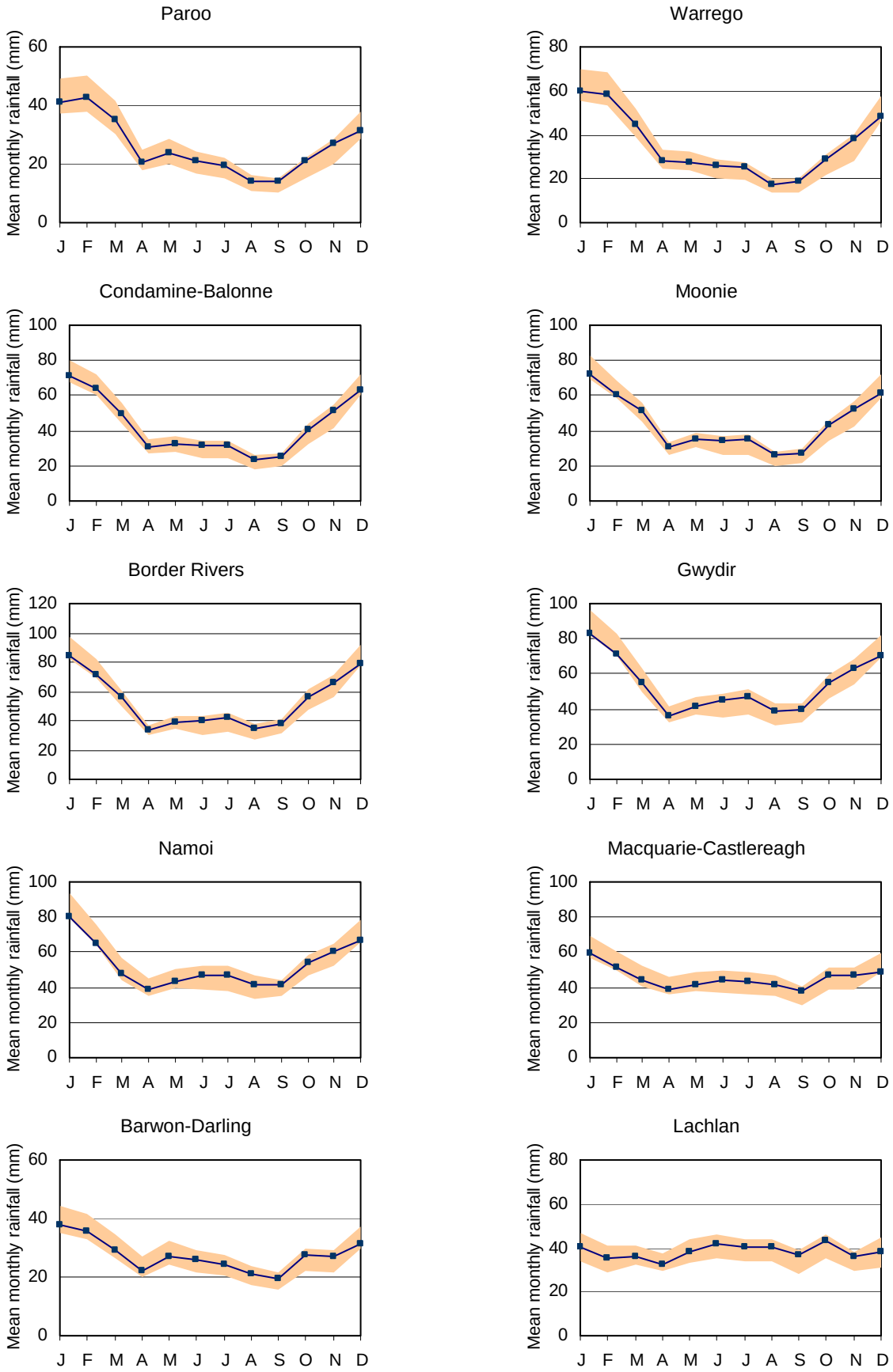

Figure 4-14. Mean monthly rainfall averaged over the each of the 18 Murray-Darling Basin regions for the historical climate, with the extreme range for future climate shown in orange

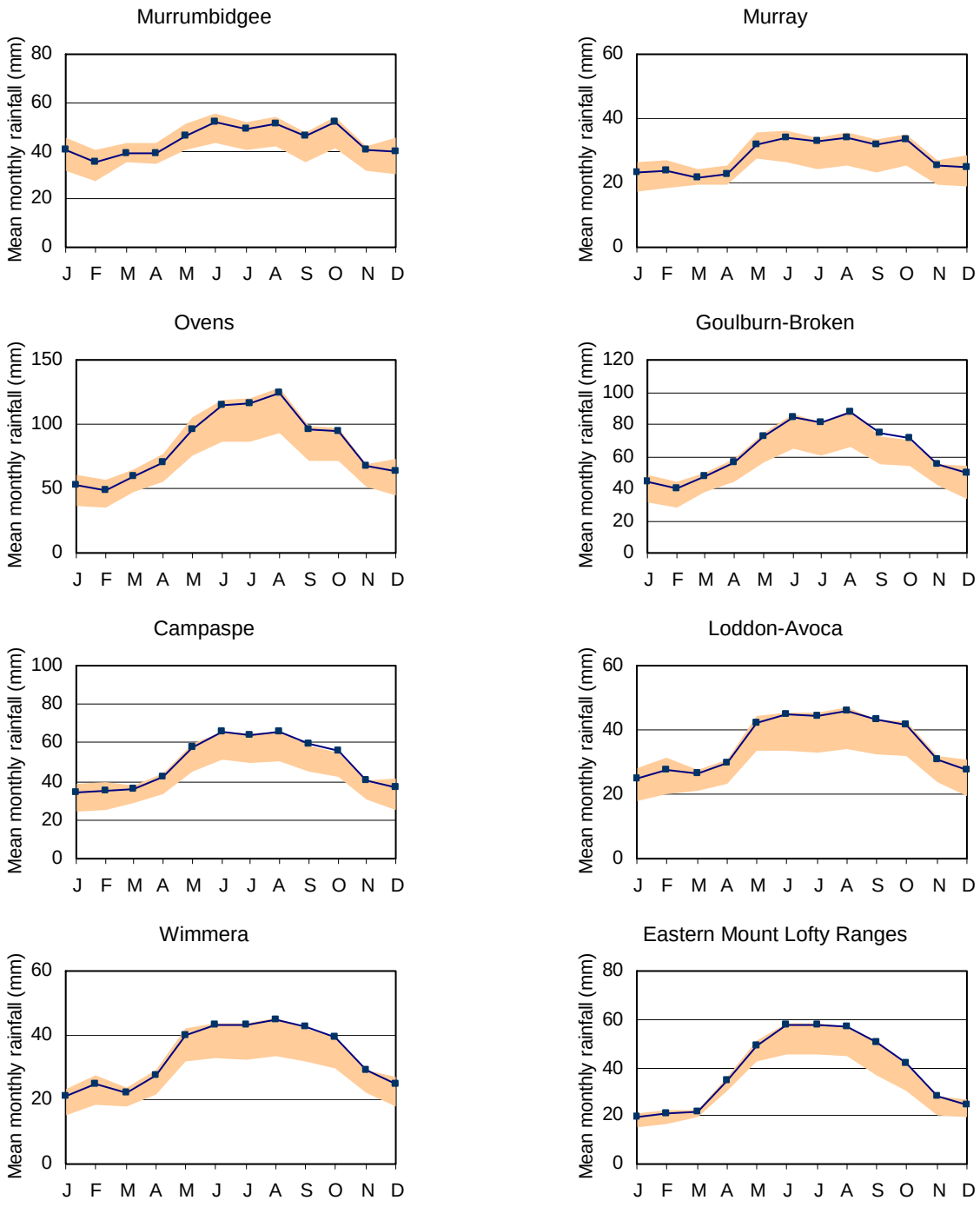

Figure 4-14 (continued). Mean monthly rainfall averaged over the each of the 18 Murray-Darling Basin regions for the historical climate, with the extreme range for future climate shown in orange

4.5 Change in future daily rainfall distribution

To account for changes in the future daily rainfall distribution, the different rainfall amounts are scaled differently. The scaling factors for the different rainfall percentiles/amounts are determined by comparing daily rainfall simulations from the 15 GCMs for a single SRES A1B run for two 20-year time slices, 2046 to 2065 and 1981 to 2000.

The method used is illustrated in Figure 4-15 using winter rainfall simulations from the CSIRO-MK3.0 GCM for two grid cells, one in south-east MDB and one in northern MDB. The plots on the left compare the 2046 to 2065 and 1981 to 2000 daily rainfall distributions, and the plots on the right show all the percent changes in 2046 to 2065 rainfall relative to 1981 to 2000 rainfall at the same daily rainfall ranks/percentiles. To obtain a smooth transition in the 'daily scaling' factors, the percent changes are estimated by averaging the rainfall amounts over percentile ranges: 1st percentile (all points smaller than 2nd percentile), 5th percentile (all points between 2.5th and 7.5th percentiles), 10th percentile (all points between 7.5th to 12.5th percentiles), and every five percentile range upwards to a highest category (see Figure 4-15), where all the small rainfall amounts are considered together. The highest category bound is defined by the percentile at which the observed rainfall is less than 1 mm, or the 30th percentile if the percentile at which the observed rainfall is less than 1 mm is above the 30th percentile. Therefore, if the highest category bound is the 30th percentile, all rainfall amounts above the 30th percentile are lumped together and used to determine the single value of percent change in rainfall amounts above the 30th percentile. The percent changes at the discrete percentile values are then interpolated to obtain the percent changes for all the rainfall percentiles/ranks (see Figure 4-15).

Each of the four seasons is considered separately. As in the estimation of the seasonal scaling factors in Sections 4.3 and 4.4, the changes for the different rainfall percentiles are expressed as a percent change per degree global warming, which are then multiplied by the change in temperature for each of the global warming scenarios for ~2030 relative to ~1990 to obtain changes for the different rainfall percentiles for the different global warming scenarios.

For each of the 15 GCMs and each of the three global warming scenarios, the above daily scaling factors are used to scale the different daily rainfall amounts in the 1895 to 2006 daily rainfall series to obtain 112 years of daily rainfall series for a ~2030 climate relative to a ~1990 climate. The entire series is then scaled, using a different constant factor for each of the four seasons, to ensure that the mean rainfalls in the four seasons are the same as those in Section 4.4 determined using the seasonal scaling factors. This is because the seasonal scaling factors are determined using a large number of data points from several ensemble runs from the archived GCM continuous monthly simulations over more than 200 years, while the archived GCM daily simulations used to estimate the daily scaling factors are available only for two time slices from limited modelling runs. In addition, because of the large spatial resolution of GCMs, the monthly simulations are more realistic than the daily simulations.

Figure 4-16 shows the number of GCMs that indicate that the future extreme daily rainfall (1st percentile rainfall or rainfall that is exceeded less than 1 percent of the time) will be more intense in summer and winter. Although more than three-quarters of the GCMs show a reduction in mean winter rainfall in the southern half of the MDB (Figure 4-10), about one-half of the GCMs indicate that the future extreme daily rainfall will be more intense (Figure 4-16).

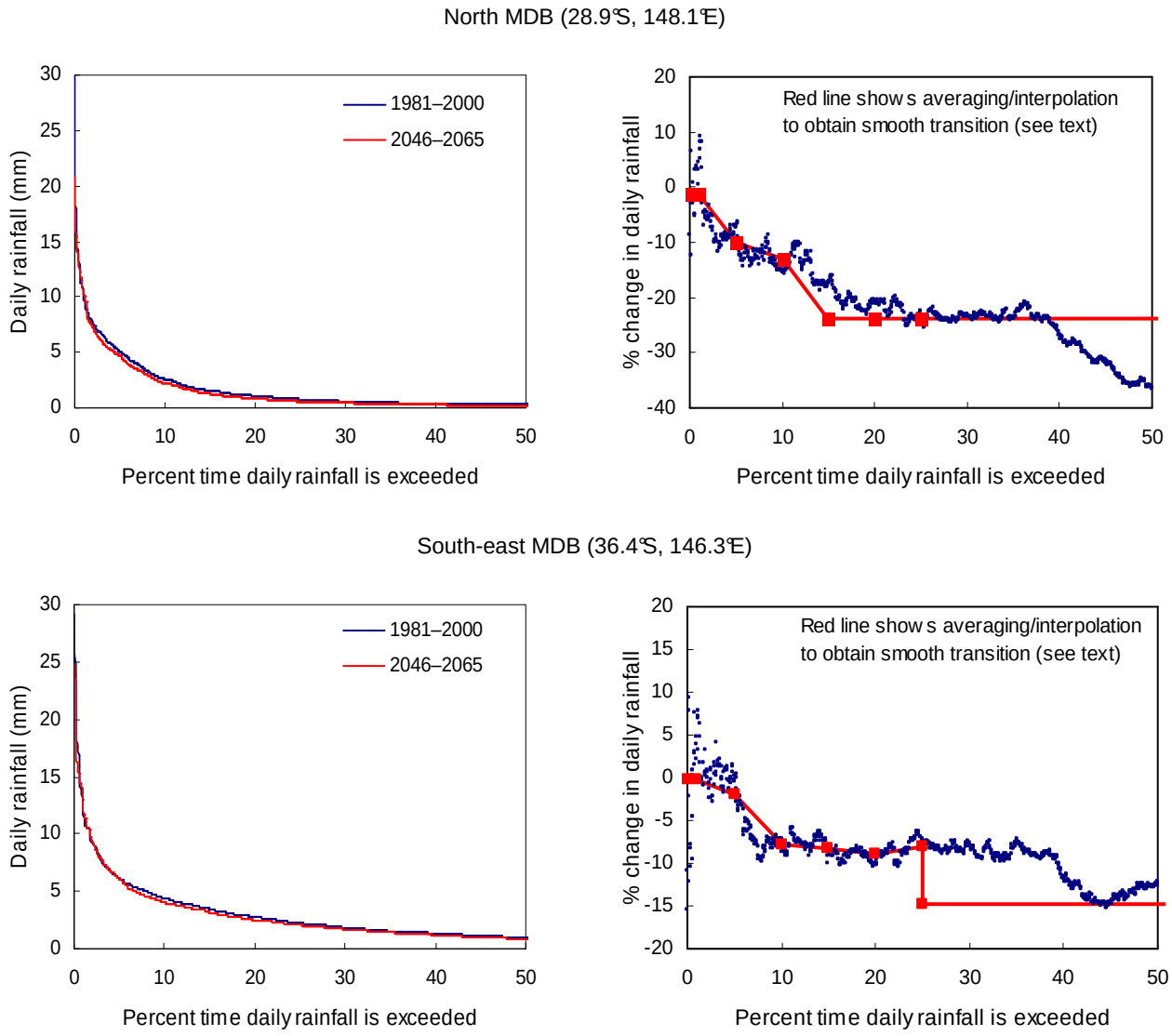

Figure 4-15. Example plots showing method used to estimate changes in the different rainfall amounts.
The left hand side plots compare the 2046–2065 and 1981–2000 daily rainfall distributions.
The right hand side plots show the percent changes in the different rainfall percentiles for 2046–2065 relative to 1981–2000.

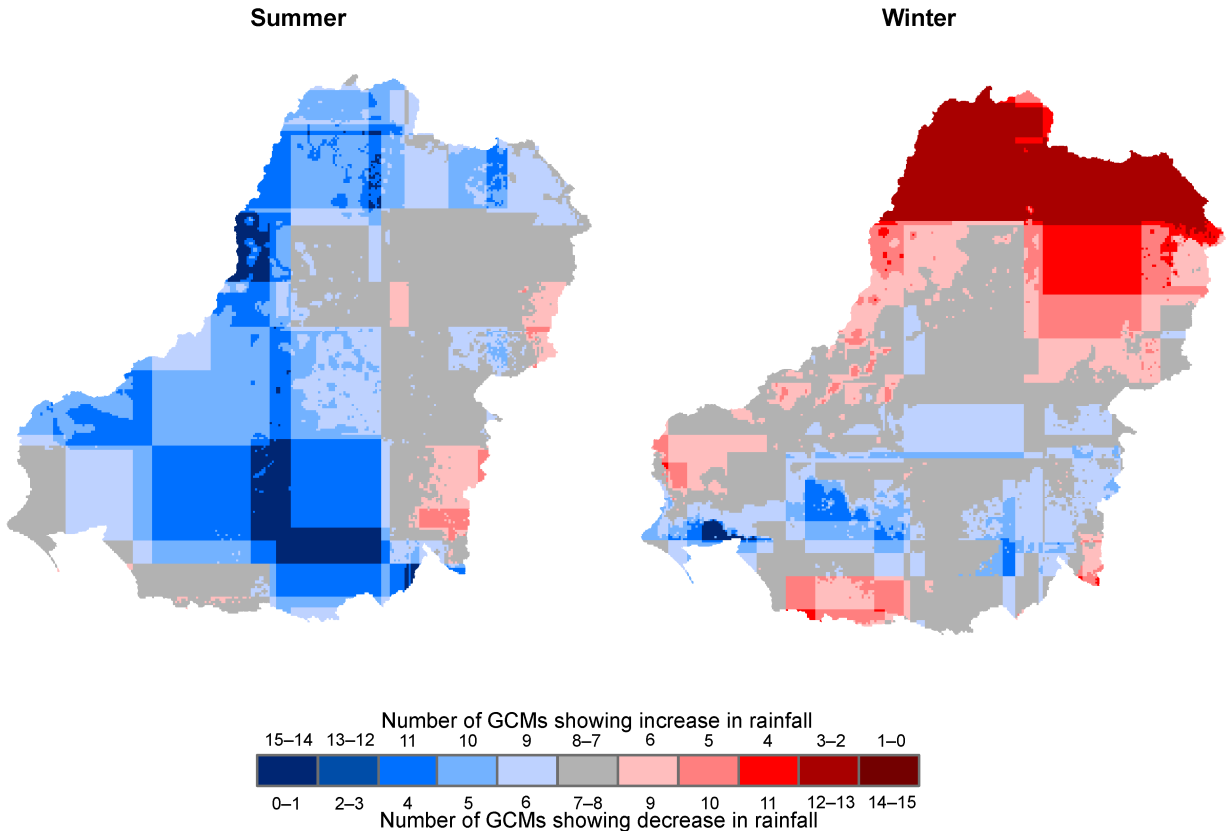

Figure 4-16. Number of global climate models showing an increase (or decrease) in future extreme daily rainfall (1st percentile rainfall) in summer (DJF) and winter (JJA) (note that all 15 global climate models are used)

5 References

Chiew FHS (2006a) An overview of methods for estimating climate change impact on runoff. 30th Hydrology and Water Resources Symposium, Launceston, Dec 2006, CDROM.

Chiew FHS (2006b) Estimation of rainfall elasticity of streamflow in Australia. Hydrological Sciences Journal 51, 613-625.

Chiew FHS and Leahy C (2003) Comparison of evapotranspiration variables in Evapotranspiration Maps of Australia with commonly used evapotranspiration variables. Australian Journal of Water Resources 7, 1–11.

Chiew FHS, Vaze J, Viney NR, Jordan PW, Perraud J-M, Zhang L, Teng J, Young WJ, Penaarancibia J, Morden RA, Freebairn A, Austin J, Hill PI, Wiesenfeld CR and Murphy R (2008) Rainfall-runoff modelling across the Murray-Darling Basin. A report to the Australian government from the CSIRO Murray-Darling Basin Sustainable Yields Project. CSIRO, Australia.

CSIRO and Bureau of Meteorology (2007) Climate change in Australia. Technical report, www.climatechangeinaustralia.gov.au.

Frost AJ, Thyer M, Kuczera G and Srikanthan R (2007) A general Bayesian framework for calibrating and evaluating stochastic models of annual multi-site hydrological data. Journal of Hydrology, http://dx.doi.org/10.1016/j.jhydrol.2007.03.023.

Frost AJ, Chiew FHS, Vaze J, Davidson A, Teng J, Wang QJ and Podger GP (2008) Stochastic hydrological modelling for the Gwydir region and Goulburn Simulation Model region. A report to the Australian government from the CSIRO Murray-Darling Basin Sustainable Yields Project. CSIRO, Australia.

IPCC (2000) Special report on emission scenarios (SRES) Special Report of the Intergovernmental Panel on Climate Change (Editors: N Nakicenovic and R Swart), Cambridge University Press.

IPCC (2007) Climate Change 2007: The Physical Basis. Contributions of Working Group 1 to the Fourth Assessment Report of the Intergovernmental Panel on Climate Change. Cambridge University Press (www.ipcc.ch).

Jeffrey SJ, Carter JO, Moodie KB and Beswick AR (2001) Using spatial interpolation to construct a comprehensive archive of Australian climate data. Environmental Modelling and Software 16, 309–330.

Jones RN, Chiew FHS, Boughton WC and Zhang L (2006) Estimating the sensitivity of mean annual runoff to climate change using selected hydrological models. Advances in Water Resources 29, 1419–1429.

Maheepala S and Perera CJC (1996) Monthly hydrologic data generation by disaggregation. Journal of Hydrology 178, 277–291.

Morton FI (1983) Operational estimates of areal evapotranspiration and their significance to the science and practice of hydrology. Journal of Hydrology 66, 1–76.

Potter NJ, Chiew FHS, Frost AJ, Srikanthan R, McMahon T, Peel MC and Austin JM (2008) Characterisation of recent rainfall and runoff across the Murray-Darling Basin. A report to the Australian government from the CSIRO Murray-Darling Basin Sustainable Yields Project. CSIRO, Australia.

Whetton P, McInnes KL, Jones RJ, Hennessy KJ, Suppiah R, Page CM and Durack PJ (2005) Australian climate change projections for impact assessment and policy application: a review. CSIRO Marine and Atmospheric Research Paper 001, www.cmar.csiro.au/e-print/open/whettonph_2005a.pdf.

WMO (2006) WMO statement on the status of the global climate in 2006. World Meteorological Organisation.

Contact Us

Phone: 1300 363 400
+61 3 9545 2176

Email: enquiries@csiro.au

Web: www.csiro.au

Your CSIRO

Australia is founding its future on science and innovation. Its national science agency, CSIRO, is a powerhouse of ideas, technologies and skills for building prosperity, growth, health and sustainability. It serves governments, industries, business and communities across the nation.